

Crinoids in Lilliput:  
Morphological Change in Class Crinoidea across the Ordovician-Silurian Boundary

A Senior Honors Thesis

Presented in Partial Fulfillment of the Requirements for graduation *with research distinction* in  
Geological Sciences in the undergraduate colleges of The Ohio State University

by

Matthew Borths

The Ohio State University  
May 2008

Project Advisor: Professor William I. Ausich, School of Earth Sciences

## Table of Contents

Figures contents .....	iii
Abstract .....	iv
Acknowledgements .....	v
Introduction .....	1
Crinoid Basics .....	2
Lilliput Effect and Cope's Rule .....	2
Paleozoic Crinoid Faunas .....	3
Sturctural History and Foreland Basin .....	5
Stratigraphy .....	6
Vaureal .....	7
Ellis Bay Fm. ....	8
Becscie Fm. ....	9
Merrimack .....	10
Gun River .....	10
Jupiter Fm. ....	10
Chicotte Fm. ....	11
Research Methods .....	12
Statistical Analysis .....	13
Results .....	14
Early vs. Middle Paleozoic Faunas .....	15
Discussion .....	16
Are the data real? .....	16
Getting Small .....	18
Ecological Implications .....	19
Conclusions .....	21
Figures (see below for details) .....	22
Appendix I (Data collected) .....	34
References .....	42

*WHEN I found myself on my feet, I looked about me, and must confess I never beheld a more entertaining prospect. The country round appeared like a continued garden, and the inclosed fields, which were generally forty foot square, resembled so many beds of flowers. These fields were intermingled with woods of half a stang, and the tallest trees, as I could judge, appeared to be seven foot high. I viewed the town on my left hand, which looked like the painted scene of a city in a theatre.*

- Jonathan Swift, *Gulliver's Travels* Part II: The Voyage to Lilliput

## Figures

Figure 1. Basic stalked-crinoid anatomy .....	22
Figure 2. Modern Feeding Crinoid .....	23
Figure 3. Crinoid Phylogeny.....	24
Figure 4. Anticosti Island Map .....	25
Figure 5. A stratigraphic column of Anticosti Island, Quebec .....	26
Figure 6 Body size range per formation. ....	27
Figure 7. Average Calyx Volume .....	28
Table 1. Mann-Whitney p-values .....	29
Figure 8. Ordovician vs. Silurian species diversity .....	30
Figure 9. Ordovician vs. Silurian volumes .....	31
Figure 10. Ordovician vs. Silurian specimens .....	32
Figure 11. Anticosti Island facies .....	33

## Abstract

The Ordovician-Silurian (O-S) transition marks the second most catastrophic mass-extinction event to impact life on Earth. A rapid global cooling event led to a glacial epoch that devastated biological communities around the world, leaving a depauperate group of survivors to diversify and repopulate the biosphere. In this project we address how members of the Crinoidea (Phylum Echinodermata) responded morphologically to the ecological stressors at the end of the Ordovician.

In addition to suffering a mass extinction and undergoing a macroevolutionary faunal change, crinoids experienced a morphological response of severe reduction in body size, an evolutionary trend recently termed “The Lilliput Effect.” To test this hypothesis, crinoids from the Ordovician-Silurian stratigraphic sections on Anticosti Island, Quebec are examined. Anticosti Island has the best-preserved shelly fossil record through this evolutionary boundary. This class-wide shrinking was documented by measuring the width and length of fossil crinoid calyxes from before, during, and after the O-S transition. These data were then used to calculate the volume of individuals. An 85% reduction in body size is documented during the mass extinction interval. Nonparametric statistics are used to demonstrate significant or not significant body size reductions through the Anticosti section. After this interval, average body volume increased by 1074%. The Lilliput Effect has been documented in more recent mass extinctions (Late Cretaceous, Late Eocene), but never observed in any group of organisms from the Paleozoic Era.

This Lilliput response does not correlate to changes in depositional environments through the Anticosti section. It is presumably a biological response to a collapse in the biosphere, but whether this is a global paedomorphic shift or a product of more local selective factors is unclear. To test this question, the manifestation of the Lilliput Effect among “winning” and “losing” crinoid clades across this macroevolutionary change is evaluated.

## **Acknowledgements**

I would like to thank the College of Arts and Sciences Honors Research Grant committee and Tiovenen Geology Scholarship committee for financial support for this project. I would also like to thank Christina O'Malley and Dr. Lawrence Krissek for discussion of crinoids and Anticosti Island and Dr. Dale Gnidovec for access to Orton Geological Museum while conducting research. Most importantly I would like to thank my research advisor, Dr. William Ausich. Dr. Ausich's discussion, advice and guidance have been instrumental in the formation of this thesis and in the formation of my own research interests in deep time and the paleontological record.

## Introduction

The Ordovician-Silurian boundary is marked by a massive faunal turnover, the second largest mass-extinction event in life's history (Sepkoski 1981). An estimated 57% of genera and 25% of families went extinct globally during this interval approximately 440 million years ago (Hallam and Wignall, 1997). Characterizing the foundation of the subsequent Middle Paleozoic ecosystem requires a close examination of the Ordovician-Silurian transition. However, the Ordovician-Silurian boundary is traditionally identified by a near-global disconformity as sea levels plummeted between 70 and 100 meters leaving vast expanses of nearshore to shallow marine sediments exposed to erosion. This rapid drop in sea level was driven by the growth of a massive southern hemisphere ice sheet that covered the paleocontinent of Gondwana, as evidenced by Upper Ordovician glacial tills and striations in the Sahara Desert, Spain, Southern France and South America (Berry and Boucot, 1973). This fall in sea level was followed by a Llandovery transgression, recognized in boundary strata around the globe (McKerrow, 1979).

Due to the common, significant unconformity at the O-S boundary, it has been historically difficult to characterize the biological response to the stresses induced by the climate change and sea level fall caused by the growth of the Gondwanan ice sheet. Most boundary sections allow only a cursory discussion of major clades that are missing or that apparently radiated. Characterizing survivorship trends is particularly difficult. The type locality for the O-S boundary is Dob's Lin, Scotland, where a deep marine facies preserves no shelly fossils and no record of how biologically dense reefs responded to the Late Ordovician crisis. This is typical for preservation normally associated with the O-S boundary. However, there is one notable locality that preserves a shelly fossil record across the boundary section: Anticosti Island, Quebec. Due to a complex tectonic and sedimentary history, Anticosti Island preserves a nearly

complete section of Upper Ordovician to Lower Silurian strata. The intact boundary section coupled with abundant tempestites throughout the section, allows a temporally constrained sequence for analyzing community-level ecological extinction and recovery through the boundary section.

### **Crinoid Basics**

The Ordovician-Silurian extinction dramatically affected the species diversity of major groups such as the graptolites, brachiopods and echinoderms (Hallam and Wignall 1997).

Crinoids are a large class of stalked echinoderms that were abundant reef builders during the Paleozoic and survived into the modern period with relatively lower diversity. These animals are suspension-feeders. Stalked crinoids anchor themselves to the substrate with a holdfast at the distal end of the stalk. This stalk supports the body of the animal, or calyx. The calyx contains the digestive tract of the animal as well as the reproductive organs. The calyx also supports the arms of the crinoid. The arms contained tube feet that are used to capture food from the water column (Figure 1). When feeding, the arms, or filtration fan, are opened perpendicular to the current, allowing water to pass through the meshwork of radiating arms, and food is captured from the water column (Hess et al. 1999)(Figure 2).

### **The Lilliput Effect and Cope's Rule**

There is little consensus on the ultimate causes of mass-extinction events in the fossil record; however, proximate causes abound. Changes in climate, salinity, habitat area and atmospheric composition are commonly recorded at or near intervals of biodiversity collapse, resulting in reduced origination rates relative to extinction rates. Concurrent with higher extinction rates, the organisms within an evolutionary lineage may “shrink” in body size. In

some cases this reduction in average body size is attributable to extinction of larger organisms that are more vulnerable to environmental change, because larger body size demands greater energetic costs. However, dwarfing during stressful environmental periods can also be a phenotypic response to new environmental conditions within a lineage. This evolutionary trend of reduced body size was named The “Lilliput Effect” in 1993 when diminished graptolite body size was found to coincide with “unfavorable growth conditions” during the Late Silurian (Urbanek 1993).

The Lilliput Effect functions as an alternative to Cope’s Rule, first proposed by Edward Drinker Cope in 1896. Cope’s rule describes the tendency for evolutionary lineages to increase body size through time (Benton 2002). Increased body size conveys a wide range of advantages including increased defense against predation, a wide range of available food sources and extended species longevity (Hone and Benton, 2004). Limitations to maximum size in a lineage include mechanical constraints (The amount of weight the chitin of an arthropod’s exoskeleton can bear, for example) and ecological constraints (the abundance of food resources available to the species, for example). Cope’s Rule has primarily been applied to amniotic evolution including pterosaurs (Hone and Benton, 2007), dinosaurs (Hone et al. 2005), and mammals (Alroy, 1998). Evidence of Cope’s Rule in invertebrates has not been as extensively documented but was proven a strong evolutionary force in extant isopod lineages (Poulin, 1995) and brachiopods during the Paleozoic (Novack-Gottshall and Lanier, 2008).

### **Paleozoic Crinoid Faunas**

Paleozoic crinoids are divided into three macroevolutionary faunas: The Early Paleozoic Aspect, the Middle Paleozoic Aspect and the Late Paleozoic Aspect. The transitions are

revolutions at high taxonomic levels, subclasses and order (Baumiller, 1994; Ausich et al. 1994). The divisions between faunas are based on taxonomic composition of global crinoid diversity.

The Early Paleozoic fauna was dominated by disparids, diplobathrids, camerates, and hybocrinids (Figure 3) and existed through the Ordovician. Anticosti Island preserves the youngest history of this fauna during the Late Ordovician. The Early Paleozoic fauna contains a wide diversity of crinoid columnal morphologies that does not continue into the Middle Paleozoic fauna (Donovan 1983 and Eckert 1988), suggesting this fauna was “experimenting” with morphological symmetry and symplectial articulations to a degree unmatched by later faunas. Peters and Ausich (2008) demonstrated that the transition from the Early to the Middle Paleozoic fauna was mediated by extinction rather than ecological changes such as predation.

After the Late Ordovician extinction, the Middle Paleozoic fauna became dominant, characterized by the cladid, monobathid and flexible subclasses. Ausich and Kammer (1987) demonstrated subclass environmental preferences in Middle Paleozoic faunas. Higher turbulence habitats tended to be dominated by advanced cladids whereas carbonate settings with moderate turbulence were dominated by monobathrid camerates and primitive cladids. Flexibles and disparids were characteristic of low turbulence environments preserved as mudstone facies. Similar environmental preferences have not been detailed in Ordovician crinoid assemblages. The Middle Paleozoic Fauna dominated through the Middle Mississippian, when it declined from the Late Osagean through the Meramecian. This changeover was due to rapid faunal turnover and was not mediated by mass extinction (Ausich et al. 1994). The Late Paleozoic macroevolutionary fauna, dominated by advanced cladids, was well established by the Late Mississippian.

Only during the Late Ordovician extinction event were Paleozoic crinoid macroevolutionary faunas immediately changed by global mass-extinction events. The decline of the Middle Paleozoic fauna occurred during rapid faunal turnover, and the Late Paleozoic fauna declined before the severe extinction pressures at the end-Permian extinction. The disassociation between crinoid macroevolutionary history and global marine macroevolutionary history suggests that paleoecological processes such as predation (i.e. the rise of jawed fishes) and competition, or physical processes such as sea-level change and habitat loss, independently affected the dominance of higher taxonomic groups over others (Ausich et al. 1994).

### **Structural History and the Foreland Basin**

Anticosti Island is a remnant of a much larger early Paleozoic sedimentary platform referred to as the Anticosti Platform. The Anticosti Platform developed as a passive margin succession along the Laurentian continental margin during the Neoproterozoic as the Iapetus Ocean opened (Waldron et al. 1998) between Laurentia and Baltica. The transition from a rifting condition to a drifting condition was examined by Stockmal et al. (1995). During collision associated with the Middle to Late Ordovician Taconic Orogeny, a foreland basin developed, which accumulated the sediments of Anticosti Island. The basin closely resembled the modern St. Lawrence Seaway. It received mixed siliciclastic-carbonate sediments, with the siliclastics derived from the Taconic Mountains. Rapid sedimentation resulted in subsidence of the crust, producing further accommodation space for sediment accumulation (Long, 2007)(Figure 4).

A distinctive carbonate formation, the Lourdes Limestone (Middle Ordovician), is easily detected in seismic surveys and records a period of relatively static sea level and reduced siliciclastic input from the exposed mainland. Above the Lourdes Limestone lies a series of

overall thinner sediments of post-Middle Ordovician age. The thinner bedding implies a more distal input of siliciclastic sediments during the Late Ordovician and Early Silurian. This observation is corroborated by an examination of the sediment itself, which is well rounded and quartz-rich, with reduced feldspar abundances (Long, 2007). The rocks presently exposed on Anticosti Island would have been deposited on the distal portion of this hypothesized foreland basin, in a setting occupied by shallow, equatorial seas, conducive to carbonate deposition but subject to the occasional influx of siliciclastic material from more shoreward environments.

Using back-stripping analysis, Long (2007) calculated the decompacted stratigraphy of the basin during the deposition of the formations exposed on Anticosti Island. Long noted a rapid increase in subsidence rates during the Late Ordovician in the Anticosti basin that could have been related to an episode of sinistral shear between North Africa and Laurentia, an observation corroborated by Stockmal et al. (1995). Subsidence of both basement rock and older Ordovician sediments (at a rate of 17.87 cm/ky) allowed the region to retain a shallow marine setting despite the rapid drop in sea level that drained most shallow marine settings elsewhere during the Late Ordovician glaciation. The basin continued to subside, although at a much slower rate (0.96 cm/ky) after this interval. The platform experienced a near balance of subsidence rates, sedimentation rates, and sea level change, allowing a nearly continuous stratigraphic record to be preserved.

### **Stratigraphy of Anticosti Island**

Today Anticosti Island sits in the Gulf of St. Lawrence between the north shore of Quebec, the Gaspé Peninsula, and Newfoundland. The 260 km long and 80 km wide island exposes a composite stratigraphic section greater than 850 m thick, composed of carbonate and

siliciclastic material that has been divided, in ascending order, into seven formations: the Vaureal, Ellis Bay, Becscie, Merrimack, Gun River, Jupiter and Chicotte (Anticosti Island Map View, Fig 5). Five other formations have been identified in the subsurface of the island (Stratigraphic Column of Anticosti Island, Fig 6). All exposed formations are from Katian (Upper Ordovician) to Llandovery (Lower Silurian) Series. The oldest sediments are along the northern margin of the island. The strata dip gently toward the south. When these sediments were deposited, the Anticosti basin was between 10° and 17° south paleolatitude and enjoyed a tropical climate (Wilde 1991) that was conducive to frequent, high energy storms (i.e. hurricanes or cyclones) during the warm season (Duke 1985).

### ***Vaureal Formation***

Ordovician (Rawtheyan stage, Katian series) in age, the Vaureal is predominantly composed of gray, interbedded micrite, calcarenite and calcareous mudstone. Approximately 275 m of the formation is exposed. A further 945 to 1027 m is present in the subsurface. The upper 552 m contain graptolites from the *Amplexograptus prominens* biozone, solidly defining this formation as Rawtheyan and, unlike other formations discussed from Anticosti Island, allows the section to be correlated with confidence globally (Long, 2007). A general shallowing trend is apparent through the formation, along with periodic hard- to firmgrounds that are commonly bioturbated. The oldest members, the Lavache, Tower, Easton and Homard, do not contain stromatoporoids, colonial corals, red algae or cyanobacterial calcimicrobes, implying that this carbonate sequence was deposited below the photic zone. The presence of *Catazyga*, a deeper water brachiopod, further supports a deep water interpretation. Hummocky cross stratification and calcarenite beds in these strata indicate deposition within storm wave base. The Battery and Mill Bay members are predominantly carbonate sequences with rare sandstone

units. Stromatoporoids become common upsection and colonial coral, red algae, and calcimicrobes appear in the upper Mill Bay member, forming the oldest photic fauna preserved on the island (Long and Copper, 1994). This shallowing event corresponds to a shallowing event connected to a late Katian glacial period with evidence preserved in the Sahara (Le Heron and Craig, 2008)

The Schmitt Creek, the youngest member of the Vaureal, contains nodular calcareous mudstone with minor thin, discontinuous laminated lime sandstones and siltstones with fewer photic organisms, evidence of a deepening phase following the Katian glacial interval (Long, 2007).

### ***Ellis Bay Formation***

As the youngest Ordovician formation on Anticosti Island, the Ellis Bay Fm contains strata with evidence of the biological responses to the environmental pressures that drove the Late Ordovician extinctions. Included in this formation is a fauna representing the Hirnantian. This is a complex of cosmopolitan brachiopods and bryozoans that apparently invaded the low latitudes from higher, more temperate latitudes, perhaps indicating a global drop in water temperature (Brenchley 1989). Lithologically, the formation is composed of gray micritic limestones interbedded with sets of calcareous mudstone layers. These micritic limestones dominate the western portion of the island and grade into micrites interbedded with mixed carbonate-siliciclastic sandstones to the east (Long and Copper, 1994). An upsection shallowing trend also characterizes the Ellis Bay Formation, with patch reefs in the upper half of the formation. The highest member of the Ellis Bay is the Laframboise Member. Ranging from 0.47 m to 8 m thick, the Laframboise Member contains oncolite-rich beds, biohermal masses of coral, stromatoporoid and algal-rich mudstones and wackestones, all indicating a much shallower

depositional environment. This is particularly noteworthy as it implies the low-diversity fauna preserved in this formation not restricted simply by physical factors of a reefal facies. In fact, similar facies in overlying units (i.e. the Jupiter Formation) contain the highest biodiversity on the island (Long, 2007).

The strata of the Ellis Bay Formation are highly bioturbated, with rare, non-continuous intraformational conglomerates and grainstones. The upper boundary of the member is controversial. The highest surface of the upper-most bed, is commonly interpreted as an erosional surface with evidence of hardground boring and blackened intertidal exposures. Minor high-luminosity spar-elements from reef cavities in this section may also indicate brief periods of exposure to fresh water (Long, 2007). Without graptolites to correlate the boundary with type localities such as Dob's Lin, the completeness of the record and the exact placement of the boundary are difficult to interpret. The *nathani* conodont zone bridges the O-S boundary and extends from the Laframboise Member (highest Ellis Bay) to the Fox Point member (lowest Becscie), implying that this erosional surface may simply be a diastem with little relevant biological information missing from the section (Long, 2007). Although some disagreement exists, for this study we recognize the Ellis Bay-Becscie contact as the Ordovician-Silurian boundary.

### ***Becscie Formation***

The Becscie Formation is assigned to the Rhuddanian stage of the Lower Silurian. If the top of the Ellis Bay Formation is a surface that experienced subaerial exposure, then the Ordovician-Silurian unconformity in other regions of the globe is shared in the Anticosti sequence (although with significantly less time lost to erosion).

The Becscie Formation is composed of gray to pale yellow micrite and calcarenite. Only two members are discussed by Long and Copper (1994). The lower is the Fox Point, which contains discontinuous grainstone and carbonate units with hummocky cross-stratification and ball-and-pillow structures. The Fox Point is also interbedded with laminated micrite and thin sets of siliciclastic rich carbonate mudstones. The Chabot Member is lithologically very similar to the Fox Point, but contains a greater abundance of grainstones and intraformational conglomerates with a storm origin, revealing an upsection shallowing trend in the Becsie Fm.

### ***Merrimack Formation***

The Merrimack is late Rhuddanian in age and records development of the middle to distal shelf depositional setting. The shelf setting had a ramp geometry (as did the rest of the Anticosti platform) with a slope of less than 10 m per km (Ausich and Copper *in press*). The Merrimack locally contains deeper-water facies that shallow toward the east of the island. Hummocky or swaley cross-stratification and abrupt lateral termination of some beds indicate that lithification of some beds was interrupted by storms (Long, 2007).

### ***Gun River Formation***

Aeronian in age, the Gun River is dominated by deep-water micrites and minor shaly units that are sparsely fossiliferous. The strata weather to a pale gray or yellow color. The formation has been divided into four informal members (Long and Copper, 1994) that are conformable with one another. Planar, massive micrites dominate the lowest members, with calcareous mudstone partings forming 5% to 10% of these members. Intraformational conglomerates are prevalent low in the formation. The higher members tend to incorporate more hummocky cross-stratification and calcarenites with gutter casts, showing the effects of storm currents and bioturbation (Long, 2007).

### ***Jupiter Formation***

The Jupiter Formation encompasses the Aeronian-Telychian boundary and is approximately 164 m to 168 m thick. It is composed of calcareous mudstone, micrite, grainstone, and minor intraformational conglomerate. The East Point Member is reefal and some members contain conglomerates with crinoidal grainstones and coral-rich limestones. Hardgrounds with bioturbated surfaces are also common (Long, 2007).

### ***Chicotte Formation***

The Upper Llandovery (Upper Telychian) Chicotte Formation is 90 m of massive to wavy, thick-bedded, crinoidal grainstone with patch reefs and local karst development, indicating local emergence. The reefs and caves that were exposed are coupled with abrupt, irregular surfaces revealing a complex history of erosional disconformities and shallow-sea deposits. These disconformities probably developed during short-lived sea-level lowstands (Derochers, 2006). These low stands were not driven by slowed subsidence or tectonic uplift but by eustatic drops in sea-level caused by waning Early Silurian glaciation (Long, 2007)

## Research Methods

In order to quantify the change in mean body size through time, and particularly between the Ellis Bay and the Becscie formations, I used the calyx as a proxy for gross body size. There are several body dimensions that could be analyzed as a proxy for overall body size including the arms, stem or holdfast. However, these elements are rarely preserved in their entirety. The calyx is a finite element and any deformation or missing plates can be easily recognized. Crinoid species can also be readily identified based on their calyx morphology.

In order to evaluate body size, two linear dimensions were recorded from each crinoid calyx. The first dimension was the maximum calyx height, measured from the intersection of the highest columnal with the base of the calyx to the independent articulation of free arms. The second dimension was the maximum diameter of the calyx, generally calculated across the point of independent articulation of the brachials (Figure 1). On some crinoids the calyx has an ellipsoidal morphology (i.e. *Fibrocrinus phragmos*) and the maximum diameter is below the level where arms become free. These dimensions were measured using two different methods depending on the scale of the specimen under scrutiny. Specimens with macroscopic morphology were measured with digital calipers to the nearest hundredth of a millimeter. Microscopic specimens were measured using an eyepiece micrometer in a binocular optical microscope.

Next, each specimen was classified as a “Cone,” “Bowl,” or “Ellipse.” Cone-shaped calyxes have a triangular vertical cross section, with relatively straight margins leading from a near point at the intersection with the stem to the maximum width near the origination of the arms. Bowl-shaped calyxes have a semi-circular cross section with rounded margins and a maximum width at the origin of the brachials. Ellipsoidal calyxes have an ellipsoidal cross

section with brachials commonly originating slightly higher than the widest diameter of the calyx.

Given the maximum calyx height, maximum calyx diameter and calyx shape, the overall volume of the calyx was approximated using the basic volume calculations for either a cone, a hemisphere, or an ellipsoid.

$$\text{Volume of a cone} = (1/3)\pi(\text{Max. Height})(\text{Max. Diameter}/2)^2$$

$$\text{Volume of a hemisphere (Bowl)} = \frac{(4/3)*\pi*(\text{Max. Diameter}/2)^3}{2}$$

$$\text{Volume of an Ellipsoid} = (4/3)*\pi*(\text{Max. Diameter}/2)^3$$

Whereas none of the calyxes precisely conformed to any of these ideal forms, abstraction to one of three morphs allowed an approximate volume to be easily calculated for a large number of specimens for comparison through time.

The volume of the calyx was calculated for 329 specimens. These specimens are every complete crinoid calyx collected from Anticosti Island as of 2007 and each was identified or verified to the species or genus level by William Ausich, consistent with Ausich and Copper (*in press*).

See Appendix I for full volume results for each calyx by specimen number and species.

### **Statistical Analysis**

The mean calyx volume for a member or formation was calculated using the volume of all specimens from that member or formation. These mean volumes were then compared using the Mann-Whitney *U* test. The Mann-Whitney *U* test is a non-parametric test for determining the likelihood that two samples of observations came from the same distribution of data. This test was used here to compare the variance in volume between each member and formation. If a

significant size decrease occurred during the end-Ordovician biotic crisis, the smallest probability (p) of identical data sets would occur between the Vaureal and the Ellis Bay formations and Ellis Bay and Becscie formations. The Ellis Bay Formation records the time when the crinoid population would have experienced the greatest extinction pressures (Ausich and Peters, 2005; Peters and Ausich, 2008). See Table 1 for all calculated p-values.

## Results

Absolute sizes for each formation are plotted on Figure 7 with the full range of body sizes shaded from the smallest individual specimen volume to the largest per formation. The Ellis Bay Formation contains the smallest individual examined in this study, *Xenocrinus rubus*, at 0.00031 mm<sup>3</sup>. Also in the Ellis Bay is the specimen with the lowest maximum volume for its formation, *Euspirocrunus gagnoni* at 515 mm<sup>3</sup>. There is a range of minimum and maximum values in the other formations, but after taking the log value of the volume it becomes obvious there are similar ranges in body size in the Vaureal, the Becscie and the Jupiter formations. The Ellis Bay Formation is an outlier.

The mean calyx volume for each formation on Anticosti Island, Quebec is shown in Figure 8. The smallest formation average volume is in the Ellis Bay at 41.75 mm<sup>3</sup>. The next smallest is in the oldest formation exposed on Anticosti Island, the Vaureal Formation, with a mean calyx volume of 331.29 mm<sup>3</sup>, followed by the Jupiter Formation at 368.83 mm<sup>3</sup>. Finally, the Becscie Formation has a mean volume of 448.43 mm<sup>3</sup>.

The Vaureal, Jupiter and Becscie formations were deposited just before and just after the biotic crisis of the Late Ordovician. Each exhibits high p-values in the Mann-Whitney *U* test when compared with each other, revealing they share comparable data sets with similar individual volumes. These formation average volumes can be viewed as “normal” whereas the

Ellis Bay is viewed as “diminished.” (Note, The mean body size of the Gun River is excluded from the discussion due to poor sampling. Only 10 individuals were measured from this formation. Of these ten specimens eight were identified as *Laurucrinus sandtopensis*. Therefore, this sample is both small and not representative for a class-wide comparison.)

### **Early versus Middle Paleozoic Faunas**

Species classified as disparids and diplobathids (taxa characteristic of the Early Paleozoic crinoid fauna, or the “Ordovician Aspect”) were compared to monobathids, cladids and flexibles (taxa characteristic of the Middle Paleozoic crinoid fauna or the “Silurian Aspect”). Species diversity in each formation (Figure 9) indicates that the Middle Paleozoic taxa were already more diverse than the Early Paleozoic taxa in the Latest Ordovician before the dwarfing of the entire fauna. Both groups exhibit reduced body sizes in the Ellis Bay and both recover “normal” body sizes after the extinction event (Figure 10). It is notable that the Middle Paleozoic groups recover in the Becscie while the Early Paleozoic Aspect actually reduce average calyx volume in the Jupiter Formation before recovering a “normal” stature in the Chicotte Formation.

The numbers of specimens are also compared (Figure 11) to understand if rare taxa are driving the diversity of Middle Paleozoic faunas. If the Middle Paleozoic Aspect was diverse but not abundant, their ecological significance may be reduced compared to less diverse but abundant Early Paleozoic species. Target collection of Anticosti Island crinoids began in 1998, and this region is considered well-sampled (Ausich 2007). The Vaureal (Latest Ordovician: Rawtheyan stage) contains comparable populations of Early and Middle representatives. After this point, the Early Paleozoic population is at least one half of all specimens. The Ellis Bay contains ten times more Middle Paleozoic specimens than Ordovician. Of all specimens in the

formation 52% are *Xenocrinus rubus* (Monobathida). A further 23% are *Dendocrinus leptos* (Cladida). These two species have the smallest body sizes in the entire sample.

The Becscie Formation contains an interesting contradiction to the noted trend of Middle Paleozoic dominance through the Early Silurian. In terms of sheer population the Early Paleozoic Aspect is more abundant. However, the Early Paleozoic Aspect in the Becscie is comprised entirely of one species, *Becsciecrinus adonis*. *B. adonis* is notable for its small body size. This contrasts with the more diverse Middle Paleozoic group.

### **Discussion**

The appearance of dwarfed crinoids on Anticosti Island coincides with the hypothesized pressures of that drove the Late Ordovician mass-extinction event - the second largest extinction in life's history. Unlike later in their history, crinoid macroevolutionary dynamics were directly affected by the global extinction pressures of this event (Ausich et al 1994). Crinoid dwarfing during a global extinction event is consistent with the definition of the Lilliput Effect and raises many questions about both the nature of the Late Ordovician environment and the morphological adaptations or exaptations required of a survivor.

### ***Are the Data Real?***

As discussed in the stratigraphic description, a variety of facies are preserved on Anticosti Island. A tentative categorization of the facies of each member inferred from various studies by Long and Copper is shown in Figure 12. Each formation contains a full assemblage array of facies. Each formation preserves a diversity of habitats that may have been more or less conducive to crinoidal communities. It is possible the shrunken crinoids may be an artifact of an isolated facies that selected for a local, small fauna. However, the coincidence of this small

fauna with the most extreme environmental pressures of the Late Ordovician would also require an explanation. Finally, the reefal and grainstone facies in the Chicotte Formation include the largest crinoids on the island (*Abacocrinus latus*). These large Chicotte crinoids occur in a similar facies as the dwarfed specimens of the Ellis Bay Formation. We hypothesize that the depositional environment was not impacting the size of the animals. Rather, the general, global environmental conditions were directly affecting the success and maximum body sizes of crinoids in separate formations.

The crinoids of the Ellis Bay Formation are clearly a mature, adult assemblage. The diminutive size of these organisms reflects a true reduction in body size, not an artifact of juvenile preservation. Juvenile organisms were collected but not included in this study. Juvenile crinoids can be recognized because the brachials of juveniles are much higher than those of adults (Brower, 1978). Small animals were collected because they are the only crinoid fossils in the Ellis Bay Formation. The Ellis Bay is recognized as the key interval of Late Ordovician fauna in the midst of mass extinction. The Ellis Bay Formation has lower crinoid abundance than the higher and lower formations. Globally the Ellis Bay has the lowest crinoid genus richness in the Hirnantian. (Peters and Ausich, 2008).

On Anticosti Island the most intense collection efforts have been focused on the Ellis bay and Becscie formations. In addition to mean body size, the absolute ranges of body volume are consistent with a smaller Ellis Bay fauna (Figure 7). The largest specimen recovered from the Ellis Bay is smaller than the maximum body size of any other formation. Thus, the dwarfed crinoids in the Ellis Bay Formation represent a real episode of reduced body size coincident with the global biotic crisis.

### *Getting Small*

A Lilliputian crinoid may be an adaptation to a less productive ocean. In the short term, large body size can be advantageous in environmentally variable conditions. Larger organisms require fewer calories per unit body mass than small organisms. However, in the long term, large body sizes are costly, requiring a higher gross intake of nutrients than smaller organisms (Hone and Benton 2005). The crinoid species of the Ellis Bay did not achieve the stature of previous species because they did not acquire sufficient nutrients to support a large body mass. This reveals that stressful conditions in Late Ordovician seas were sustained through numerous generations, driving a macroevolutionary body size reduction as new species evolved to cope with new environmental conditions.

Lower productivity of the Late Ordovician ocean was driven by the sudden reduction of shallow continental seas which were vast regions of water within the photic zone. With the recession of these seas and the global reduction of primary producers, the shallow ecosystem collapsed. The lower abundance of biomass would produce less particulate food for crinoids.

There are two life-history strategies that would produce the diminutive body sizes observed in the Ellis Bay Formation. First, surviving crinoids may have retained an ancestral life-history with the intervals of maturation and reproduction equal to ancestral, unstressed organisms. The expression of small body size would then reflect a reduced food supply. A paucity of nutrients simply would not allow an animal to achieve its maximum potential body size, producing a group of stunted adult animals. This was the scenario first proposed by Urbaneck to explain the Lilliput Effect in graptolites. The animals were stunted by a nutrient-poor ocean.

The alternative to conserved generation time, is a paedomorphic trend in all Late Ordovician crinoids to size reduction. The survivors of the biotic crisis and denizens of the Ellis Bay could have accelerated the onset of sexual maturity over many generations, reproducing before they achieved a larger stature, increasing generation rates. The first model (The Slow Maturation Model) suggests the same number of generations occurred in the same unit time in the Ellis Bay and the Vaureal. The second (The Rapid Reproduction Model) suggests more generations of crinoids were produced in the same unit time in the Ellis Bay than in the Vaureal.

We suggest that the Rapid Reproduction Model is supported by this study. The Slow Maturation Model would not necessarily produce the new species observed in the Ellis Bay with derived morphologies relative to their ancestors. Species stunting would have produced an Ellis Bay fauna that was morphologically identical to the Vaureal except with smaller body sizes.

The Rapid Reproduction Model would allow for rapid macroevolutionary change and speciation. A greater number of generations per unit time allows a greater number of mutations and variation in less time, creating opportunities for rapid adaptation to variable environmental conditions.

### ***Ecological Implications***

Regardless of the life history strategy that facilitated the observed body sizes of crinoids on Anticosti Island, there are profound implications of a smaller, less diverse crinoid fauna in Paleozoic oceans. Crinoids have become a classic example of ecological niche partitioning through tiering. In diverse crinoid communities, different species will have different stem lengths, reducing interspecific competition for suspended food resources (Ausich 1980). Competition can be further reduced with species specialization for feeding on different sized food particles (Hess et al. 1999). The more diverse the crinoid fauna, the more tiering and

feeding specialization will occur. The dwarfed crinoid fauna is relatively diverse (Figure 9) containing 2 more species than the Vaureal Formation. However, morphologically the crinoids presumably did not achieve the heights of larger, Vaureal crinoids. Small body size puts the less abundant crinoids closer to the substrate, where food tends to be most dense but where competition with other small crinoids and other sessile, suspension-feeders, such as bryozoans and brachiopods, would be most fierce. In a stressed environment, interspecies competition is apparently increased causing a further reduction in diversity, as limited niche space is occupied by a limited number of surviving species.

The low diversity and abundance of crinoids during the Late Ordovician mass-extinction further supports the Ausich et al. (1994) hypothesis that extinction near the O-S boundary was driven more by physical factors than biological factors. Physical conditions such as water depth, temperature and circulation were driving the degradation of the ecosystem more rapidly than biological factors such as predation and competition. Only after the survivors achieved a reduced body size would the biological factors, such as competition, drive further selection and survivorship. The survivors of the second largest mass-extinction event fundamentally affected the composition of Silurian ecosystems and beyond.

## Conclusions

1. The Ellis Bay Formation contains evidence of a distinct crinoid fauna that has a statistically significant smaller body size than previous or subsequent crinoid faunas. Reduced body size co-occurs with plummeting Late Ordovician sea levels and the environmental stress induced by a rapid, severe reduction of shallow habitats and climate cooling.
2. This study marks the oldest reported incidence of the Lilliput Effect, establishing the trend as coincident with the first of the “Big Five” mass-extinction events.
3. Middle Paleozoic characteristic taxa were already dominant on the Late Ordovician reefs of Anticosti Island.
4. Middle Paleozoic dominance was not established by a more successful adaptation to diminutive body size, although a more rapid recovery of size may have allowed cladids, monobathids and flexibles to seize on large-bodied niches formerly occupied by the morphologically diverse Early Paleozoic crinoid fauna.

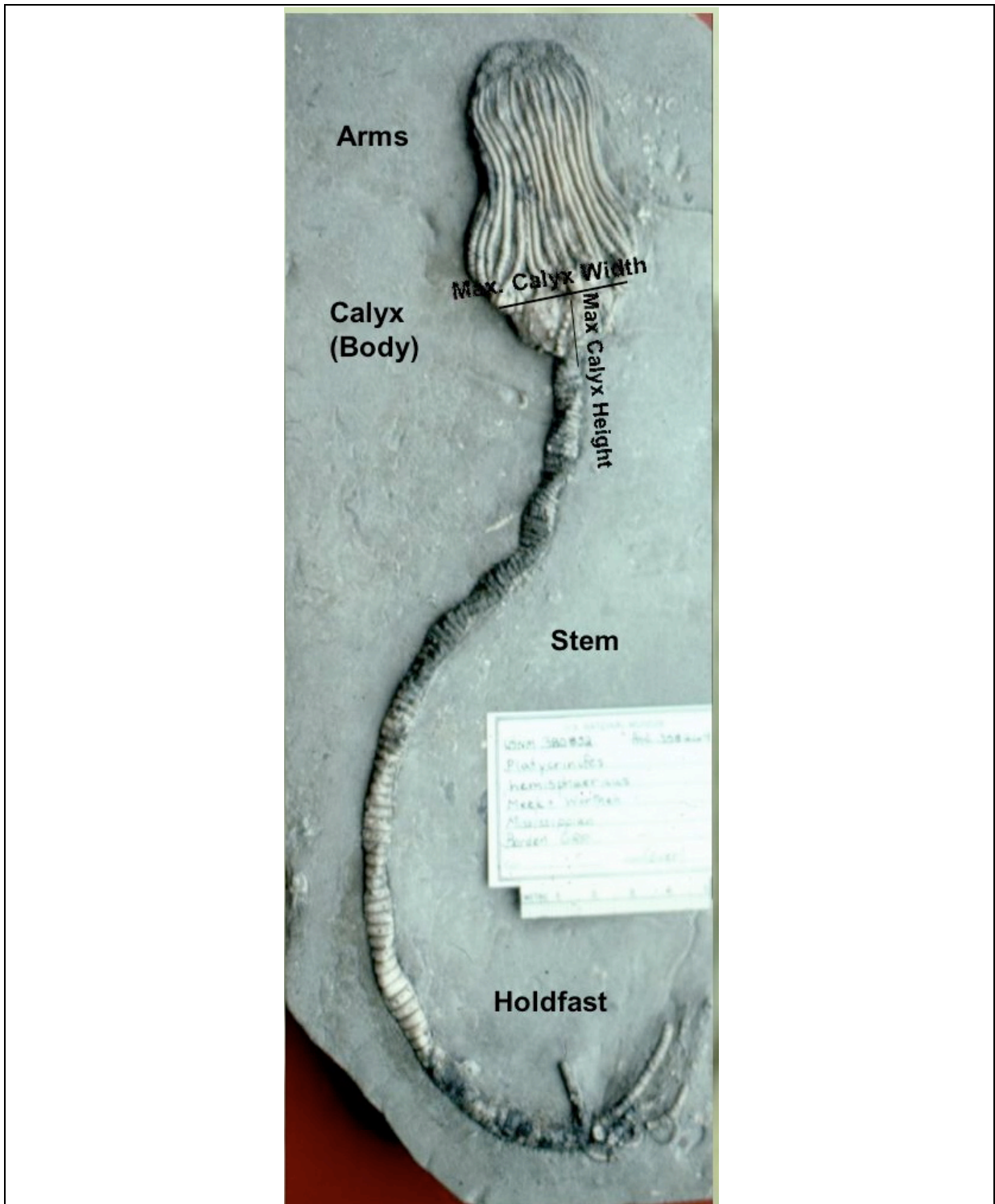


**Figure 1. Basic stalked crinoid anatomy.** The holdfast anchors the animal to the substrate so it can position the feeding fan in the water column. Food captured on the arms is passed to the central calyx where the food is digested and later excreted from the anus, which is positioned in the middle of the calyx. This figure also details the two linear dimensions used in this study to quantify calyx volume (Photo courtesy of Ausich).

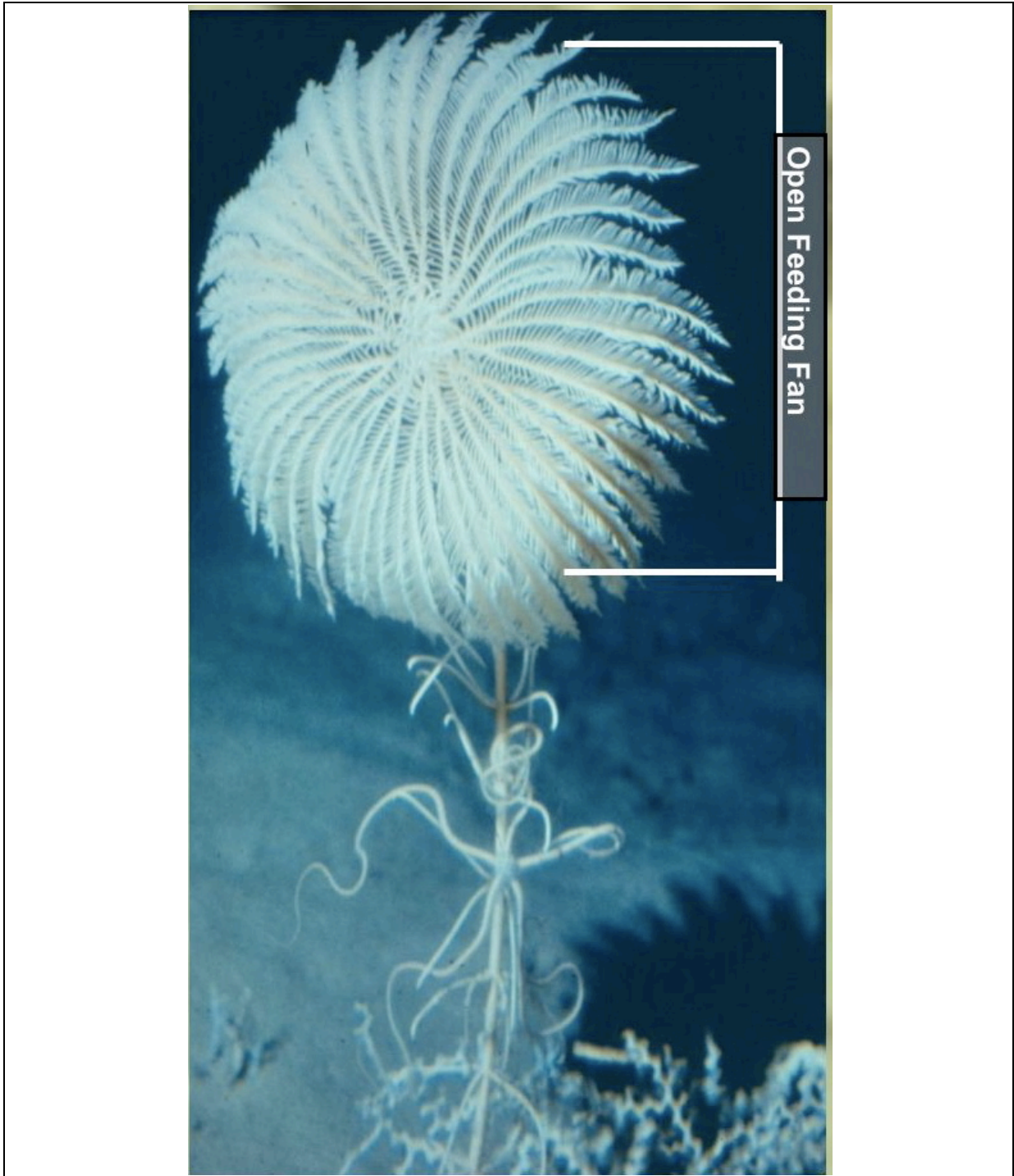


**Figure 2. A modern stalked crinoid in feeding position. The current is moving obliquely from the right back to the left front. Particulate organic material is being captured by the tube feet that cover the radiating arms. Note the ophiuroids clinging to the crinoid stalk (Photo courtesy of D.L. Meyer)**

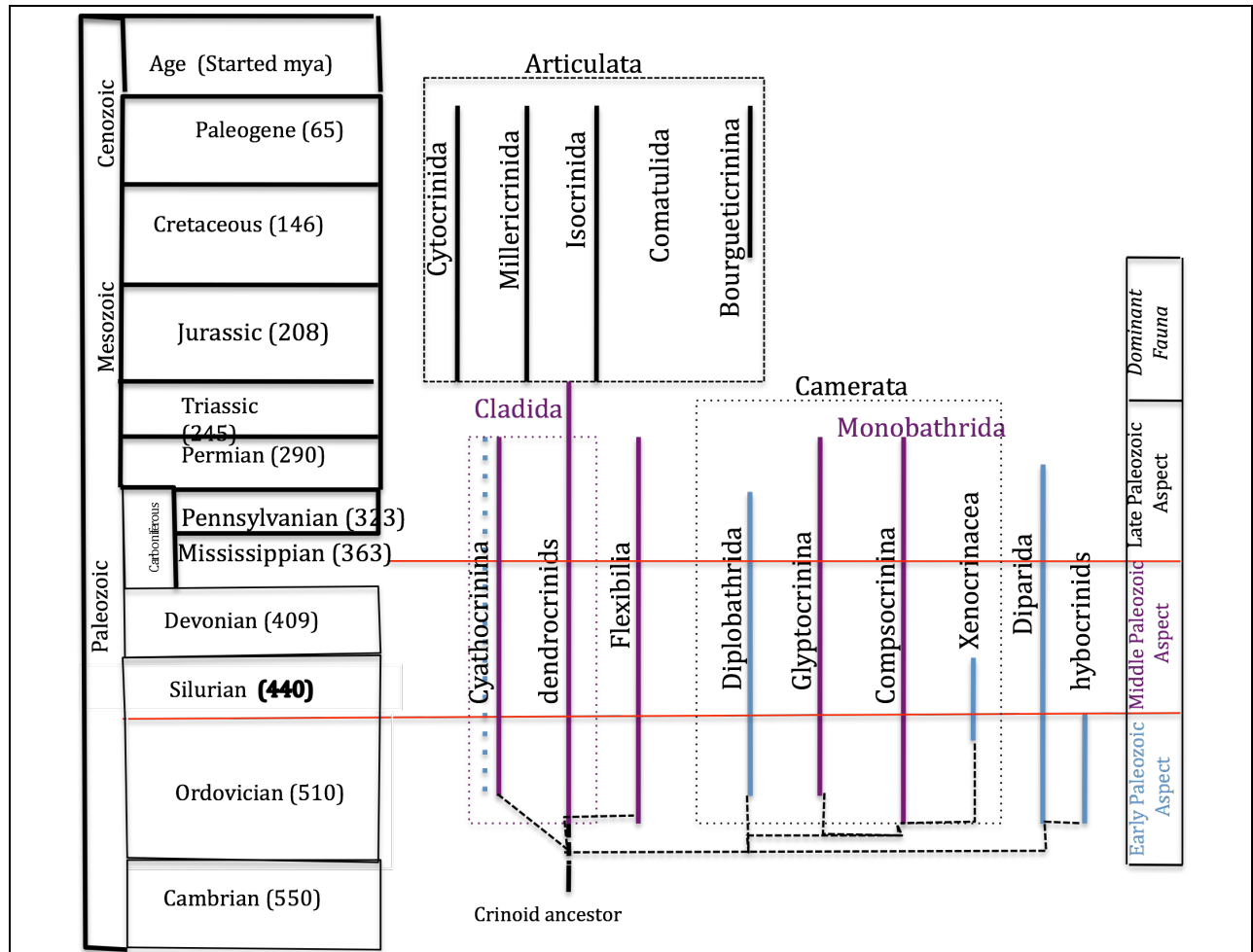


**Figure 3. Stratigraphic distribution and possible phylogeny of crinoids adapted from Simms in Hess et al. 1999. Note disparids, diplobathrids, camerates, and hybocrinids of the Ordovician Aspect coexisted with cladid, monobathrid and flexible subclasses of the Silurian Aspect fauna through most of the Paleozoic. However, which Aspect dominates determined the divisions into Early, Middle and Late Paleozoic Crinoid Faunas.**

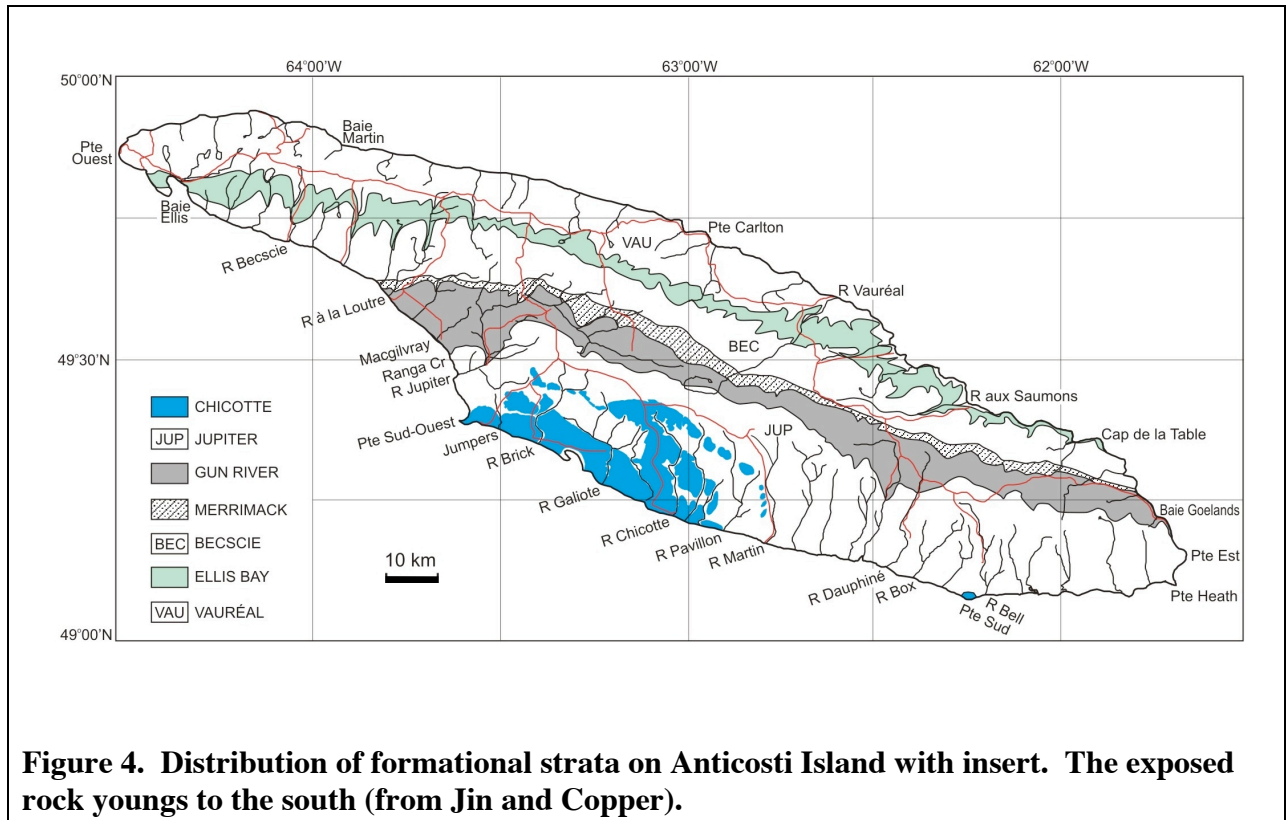


**Figure 4. Distribution of formational strata on Anticosti Island with insert. The exposed rock youngs to the south (from Jin and Copper).**

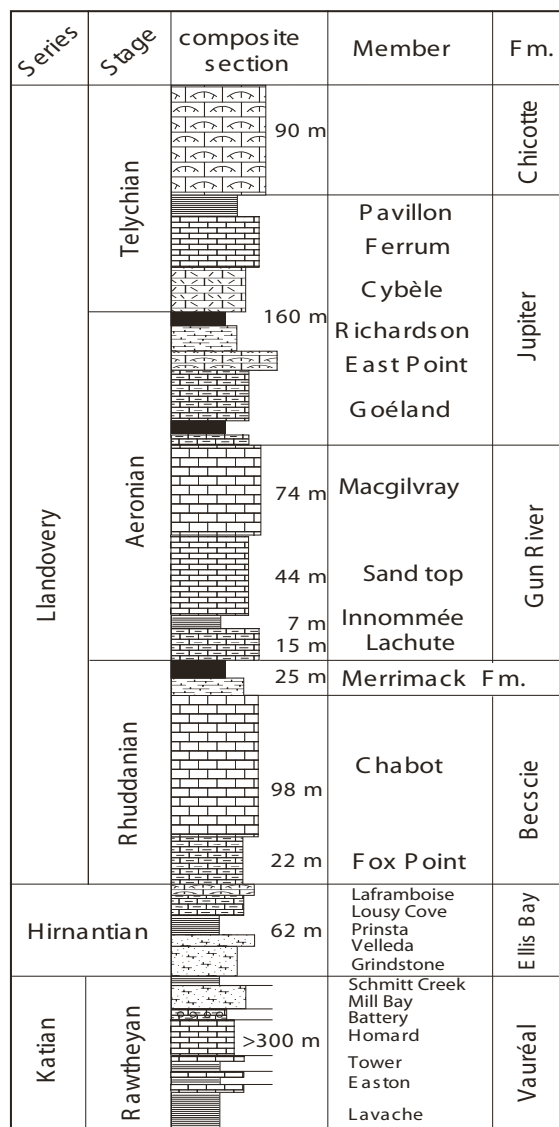
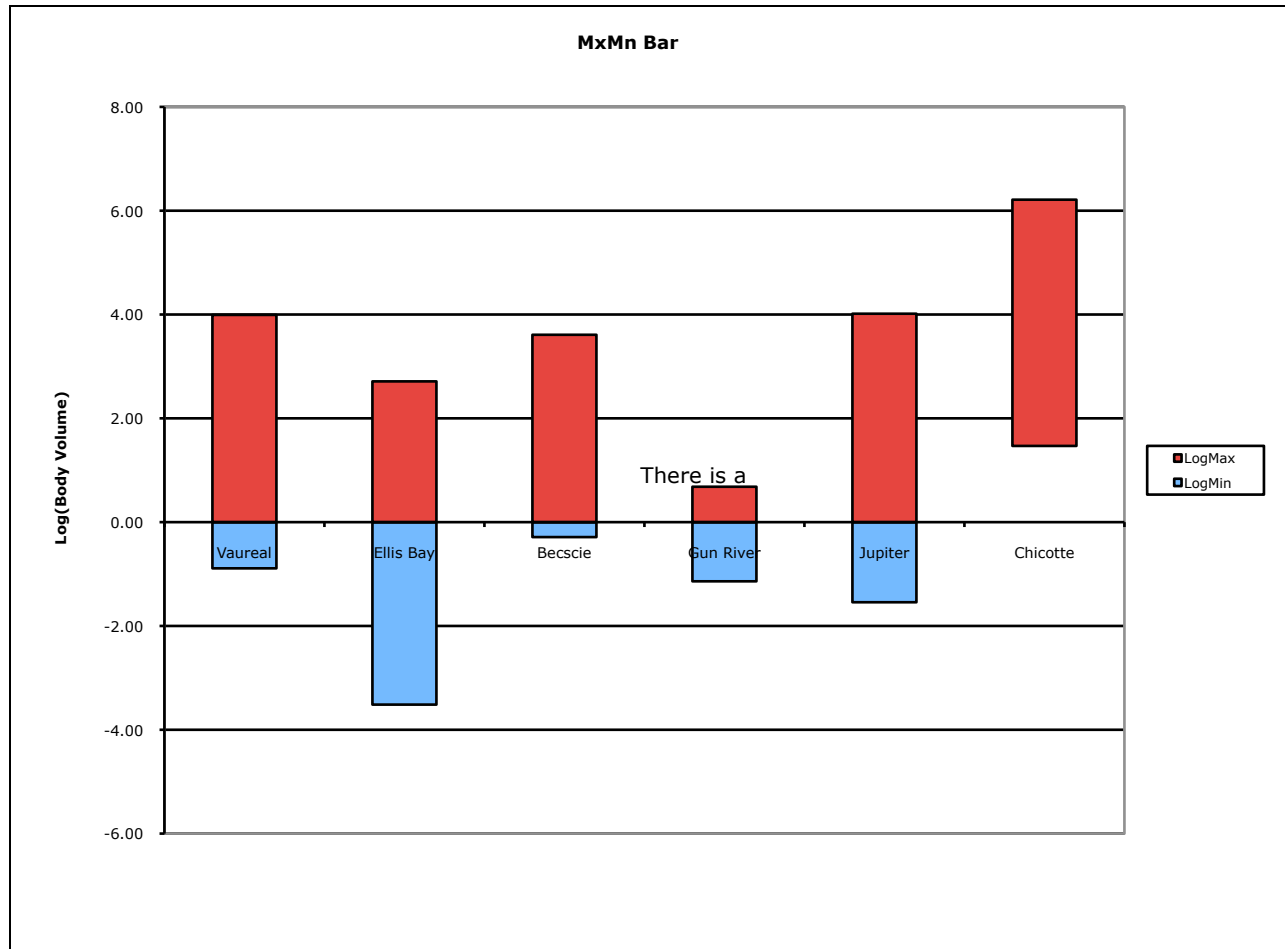


**Figure 5. A stratigraphic column of Anticosti Island, Quebec. The column depicts both exposed and subsurface formations. The Ordovician-Silurian boundary occurs between the Ellis Bay and Becschie formations (Jin and Copper).**



Formation	Min	Max	LogMin	LogMax
Vaureal	0.12	9832.48	-0.89	3.99
Ellis Bay	0.00031	515.02	-3.52	2.71
Becscie	0.52	4071.01	-0.29	3.61
Gun River	0.072	4.81	-1.14	0.68
Jupiter	0.029	10363.35	-1.54	4.02
Chicotte	29.39	55479.49	1.47	4.74

**Figure 6. Body size range of individuals per formation. Absolute smallest adult individuals are plotted along with absolute largest individuals. The Ellis Bay contains the smallest individual measured and the formation contains the smallest maximum body size of all the formations. This suggests all survivors adapted to a reduced body size strategy, rather than the small Vaureal fauna simply surviving. Macroevolutionary change is occurring in the Late Ordovician among crinoids.**

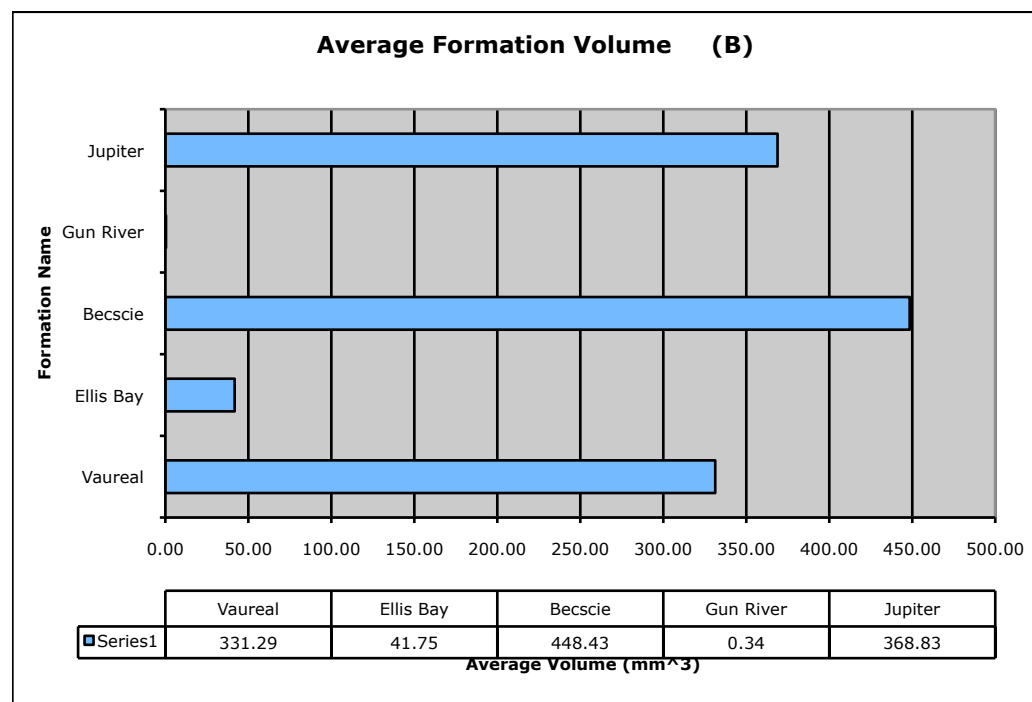
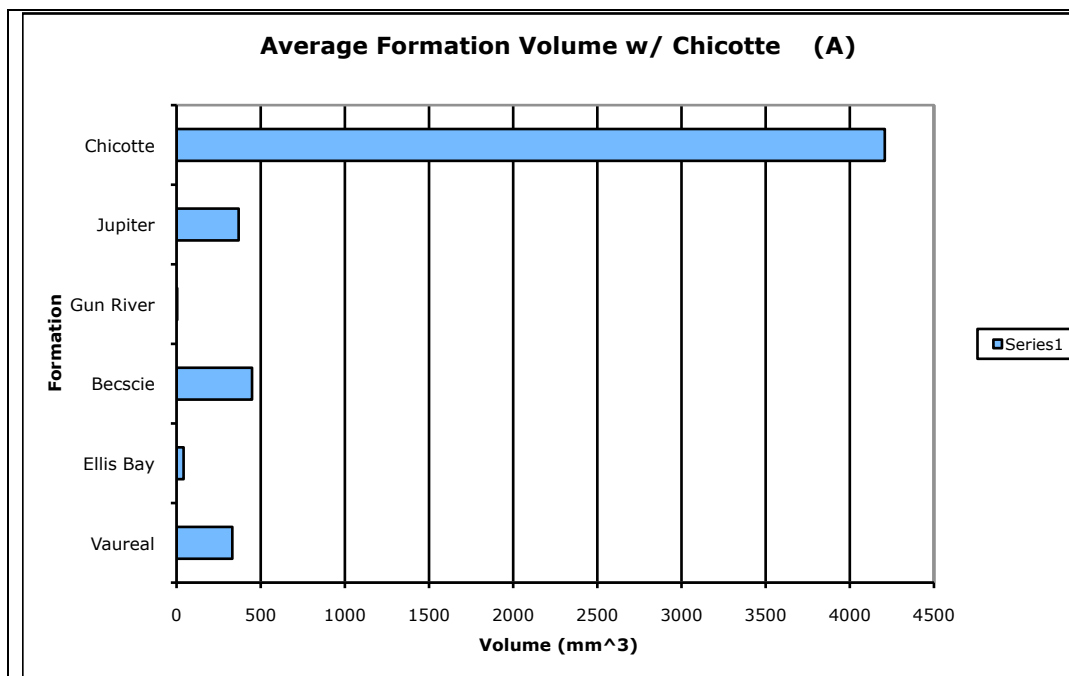


**Figure 7. The average calyx volume in each formation with the oldest formation (Vaureal) at the bottom and the youngest (Chicotte or Jupiter) at the top. Histogram A includes the Chicotte which is excluded from B to better illustrate the immediate reaction to the Late Ordovician biotic crisis. The Ellis Bay was deposited during the crisis. The reduction of average body size is interpreted by the author as a morphological response to this crisis.**

<b>Formation</b>	N	T=Ub	p(same)
Vaureal	90	822	4.16E-08
Ellis Bay	44		
Ellis Bay	44	321.5	0.004423
Becscie	25		
Vaureal	90	978	0.3205
Becscie	25		
Becscie	25	1086	0.05617
Jupiter	115		
Jupiter	115	550	2.07E-12
Chicotte	39		

**Table 1. Table showing p-values between formations. The closer a value to zero, the less-likely they share a data set. The smallest values are between the Vaureal and Ellis Bay, when the crinoids shrink, and between the Ellis Bay and the Becscie when the fauna recovers a normal stature and diversity. The Ellis Bay fauna are morphologically differentiated from their ancestors or progeny who were removed from the pressures of survivorship. It is important to note the Chicotte has generally been disregarded along with the Gun River. The size of several species of crinoid dramatically affects the average formation volume.**

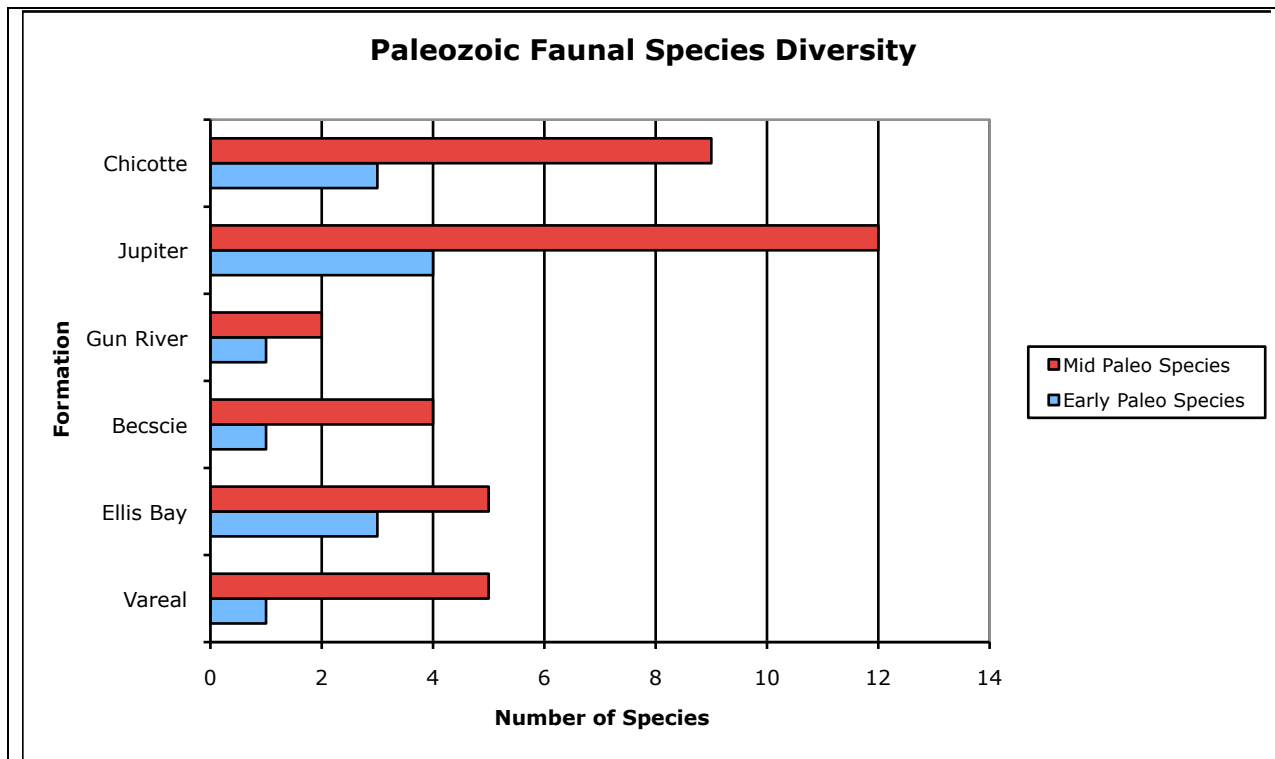
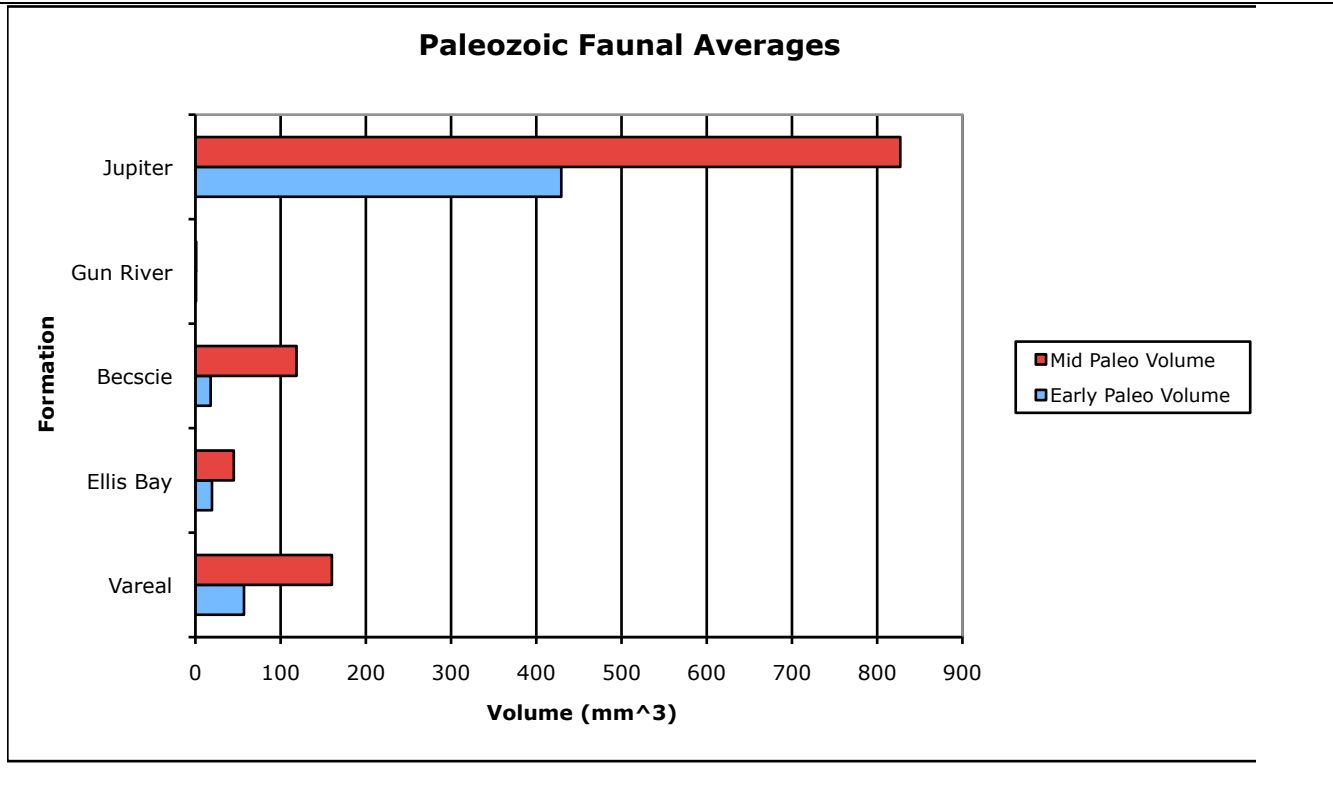


**Figure 8. Crinoid species diversity of Early Paleozoic (Ordovician Aspect) compared to the species diversity of the Middle Paleozoic (Silurian Aspect). The Silurian aspect is consistently more diverse than the Ordovician, even in the Late Ordovician suggesting the shift between dominant aspects was occurring before the biotic crisis**



Formation	Early Paleo Species	Early Paleo Volume	Early Paleo Specimens	Mid Paleo Species	Mid Paleo Volume	Mid Paleo Specimens
Vareal	1	57.00	39	5	160.14	46
Ellis Bay	3	19.46	4	5	45.02	40
Becscie	1	17.90	10	4	118.66	9
Gun River	1	0.34	1	2	0.95	9
Jupiter	4	429.33	31	12	827.13	82
Chicotte	3	19732.44	3	9	3381.70	36

**Figure 9. Average calyx volume broken down into Ordovician and Silurian aspects. Although the Silurian Aspect of the fauna is consistently larger than the Ordovician, the two groups respond in similar morphologic ways to the biotic crisis by reducing gross calyx volume. The Ordovician aspect does not immediately recover in the Becscie as the Silurian aspect recovers. This faster recovery may be one of the key factors that lead to the later dominance of the Silurian Aspect (the cladids, monobathids and flexibles) in the Middle Paleozoic.**

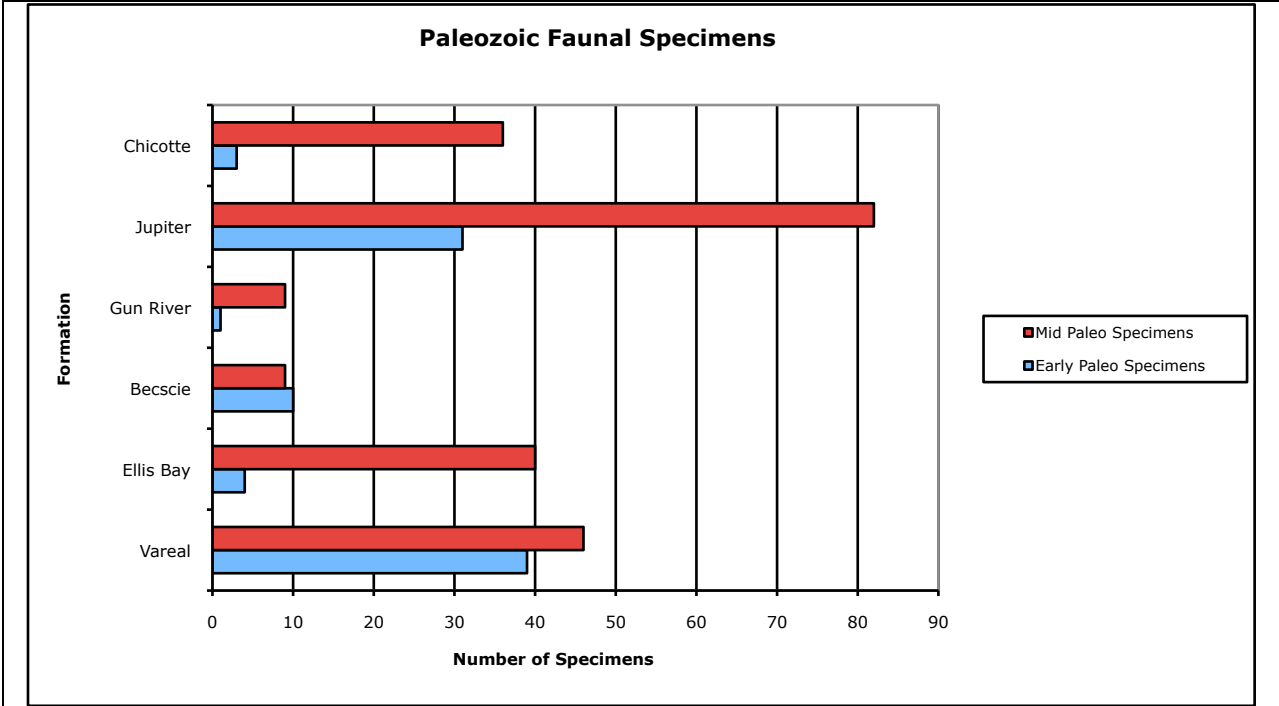


**Figure 10. The number of specimens of the Ordovician versus Silurian Aspect. The Ordovician Aspect clearly never recovers the total population density it had in the Vaureal, whereas the Silurian Aspect clearly adapts and radiates more successfully than before the Late Ordovician biotic crisis.**

System	Stage	Formation	Member	Clorida-Triples1a	atrypid-Stricklandia	Pentamerus	Colonial Corals	Reefal
S I L U R I A N	T	Chicotte						
	E							
	L	J	Pavillion					
	E	u	Ferrum					
	C	p	Cybele					
	A	l	Richardson					
	E	t	East Point					
	R	er	Goeland					
	O	G	Macgilvray					
	N	u	Sandtop					
	I	n	Innommee					
	A	R	Lachute					
	R		Merrimack					
	H U	H	Becscie	Chabot				
U		Foxpoint						
O R D O V I C I A N	H	E	Laframboise					
	I	l B	Lousy Cove					
	R		Prinsta					
	N	i y	Velleda					
	A	s	Grindstone					
	V	V	Schmidt Ck					
	R	a u	Mill Bay					
	A		Joseph Point					
	W	r	Homard					
	T	e	Tower					
H	a	Easton						

**Figure 11. Hypothesized facies of every member exposed on Anticosti Island. Each formation contains a diversity of facies. The shift to a small body size is not connected to a unique facies. Instead the trend to diminished body size is more closely connected to global events affecting the biosphere rather than local changes in water depth or reef development.**

# Appendix 1

CRINOID	SPECIMEN NUMBER	FORMATION	MEMBER	CONE/ BOWL/ ELLIPS.	Max. Calyx Height (mm)	Max. Calyx Width (mm)	Volume Estimate (mm <sup>3</sup> )	Order	Subclass	Char. Fauna
<i>Gaurocrinus limbriatus</i>	GSC 126656	Vaureal	La Vache	Bowl	7.32	11.66	415.02	Diplobathrida	Camerata	Early Paleo
<i>Gaurocrinus limbriatus</i>	GSC 126657a	Vaureal	La Vache	Bowl	1.2	2.22	2.86	Diplobathrida	Camerata	Early Paleo
<i>Gaurocrinus limbriatus</i>	GSC 126658a	Vaureal	La Vache	Bowl	3.27	4.9	30.8	Diplobathrida	Camerata	Early Paleo
<i>Gaurocrinus limbriatus</i>	GSC 126658b	Vaureal	La Vache	Bowl	5.03	5.72	49	Diplobathrida	Camerata	Early Paleo
<i>Gaurocrinus limbriatus</i>	GSC 126658c	Vaureal	La Vache	Bowl	4.1	5.93	54.59	Diplobathrida	Camerata	Early Paleo
<i>Gaurocrinus limbriatus</i>	GSC 126658d	Vaureal	La Vache	Bowl	1.66	4.08	17.78	Diplobathrida	Camerata	Early Paleo
<i>Gaurocrinus limbriatus</i>	GSC 126658e	Vaureal	La Vache	Bowl	3.61	5.84	52.14	Diplobathrida	Camerata	Early Paleo
<i>Gaurocrinus limbriatus</i>	GSC 126658f	Vaureal	La Vache	Bowl	2.14	7.83	125.68	Diplobathrida	Camerata	Early Paleo
<i>Gaurocrinus limbriatus</i>	GSC 126658g	Vaureal	La Vache	Bowl	2.39	3.07	7.58	Diplobathrida	Camerata	Early Paleo
<i>Gaurocrinus limbriatus</i>	GSC 126658h	Vaureal	La Vache	Bowl	2.51	4.68	26.84	Diplobathrida	Camerata	Early Paleo
<i>Gaurocrinus limbriatus</i>	GSC 126658i	Vaureal	La Vache	Bowl	1.3	3.73	13.59	Diplobathrida	Camerata	Early Paleo
<i>Gaurocrinus limbriatus</i>	GSC 126659a	Vaureal	La Vache	Bowl	1.97	6.45	70.16	Diplobathrida	Camerata	Early Paleo
<i>Gaurocrinus limbriatus</i>	GSC 126659b	Vaureal	La Vache	Bowl	0.66	0.79	0.13	Diplobathrida	Camerata	Early Paleo
<i>Gaurocrinus limbriatus</i>	GSC 126659d	Vaureal	La Vache	Bowl	0.92	2.89	6.35	Diplobathrida	Camerata	Early Paleo
<i>Gaurocrinus limbriatus</i>	GSC 126659e	Vaureal	La Vache	Bowl	2.52	7.07	92.52	Diplobathrida	Camerata	Early Paleo
<i>Gaurocrinus limbriatus</i>	GSC 126660b	Vaureal	La Vache	Bowl	5.53	3.16	8.24	Diplobathrida	Camerata	Early Paleo
<i>Gaurocrinus limbriatus</i>	GSC 126660c	Vaureal	La Vache	Bowl	1.71	4.61	25.57	Diplobathrida	Camerata	Early Paleo
<i>Cupulocrinus latibrachiatus</i>	GSC 126660d	Vaureal	La Vache	Cone	3.71	6.44	40.28	Dendrocrinida	Cladida	Mid Paleo
<i>Plicodendrocrinus epineffensis</i>	GSC 126660e	Vaureal	La Vache	Ellipse	5.41	5.33	79.28	Dendrocrinida	Cladida	Mid Paleo
<i>Gaurocrinus limbriatus</i>	GSC 126661a	Vaureal	La Vache	Bowl	2.95	4.81	29.13	Diplobathrida	Camerata	Early Paleo
<i>Gaurocrinus limbriatus</i>	GSC 126661b	Vaureal	La Vache	Cone	1.84	3.95	7.51	Diplobathrida	Camerata	Early Paleo
<i>Gaurocrinus limbriatus</i>	GSC 126661d	Vaureal	La Vache	Cone	5.37	4.18	24.56	Diplobathrida	Camerata	Early Paleo
<i>Gaurocrinus limbriatus</i>	GSC 126661f	Vaureal	La Vache	Cone	3.53	3.78	13.2	Diplobathrida	Camerata	Early Paleo
<i>Gaurocrinus limbriatus</i>	GSC 126661g	Vaureal	La Vache	Bowl	6.54	7.64	116.75	Diplobathrida	Camerata	Early Paleo
<i>Gaurocrinus limbriatus</i>	GSC 126661h	Vaureal	La Vache	Bowl	2.62	3.88	15.29	Diplobathrida	Camerata	Early Paleo
<i>Cupulocrinus latibrachiatus?</i>	GSC 126661i	Vaureal	La Vache	Cone	7.4	7.04	96.02	Dendrocrinida	Cladida	Mid Paleo
<i>Plicodendrocrinus epineffensis</i>	GSC 126661j	Vaureal	La Vache	Ellipse	8.16	6.05	116.1	Dendrocrinida	Cladida	Mid Paleo
<i>Pleurocystites anticostiensis</i>	GSC 126661k	Vaureal	La Vache	Ellipse	26.54	25.71	8998.25			
<i>Gaurocrinus limbriatus</i>	GSC 126662a	Vaureal	La Vache	Bowl	2.23	3.21	8.66	Diplobathrida	Camerata	Early Paleo
<i>Gaurocrinus limbriatus</i>	GSC 126663b	Vaureal	La Vache	Bowl	2.1	4	16.76	Diplobathrida	Camerata	Early Paleo
<i>Cupulocrinus latibrachiatus</i>	GSC 126664	Vaureal	La Vache	Cone	4.91	5.58	40.02	Dendrocrinida	Cladida	Mid Paleo
<i>Cupulocrinus latibrachiatus</i>	GSC 126665a	Vaureal	La Vache	Cone	5.38	6.33	56.44	Dendrocrinida	Cladida	Mid Paleo
<i>Cupulocrinus latibrachiatus</i>	GSC 126665b	Vaureal	La Vache	Cone	5.3	6.18	52.99	Dendrocrinida	Cladida	Mid Paleo
<i>Cupulocrinus latibrachiatus</i>	GSC 126665c	Vaureal	La Vache	Cone	4.82	5.14	33.34	Dendrocrinida	Cladida	Mid Paleo
<i>Cupulocrinus latibrachiatus</i>	GSC 126665d	Vaureal	La Vache	Cone	4.85	5.26	35.13	Dendrocrinida	Cladida	Mid Paleo
<i>Cupulocrinus latibrachiatus</i>	GSC 126665e	Vaureal	La Vache	Cone	3.99	5.17	27.92	Dendrocrinida	Cladida	Mid Paleo
<i>Cupulocrinus latibrachiatus</i>	GSC 126665f	Vaureal	La Vache	Cone	3.93	5.41	30.11	Dendrocrinida	Cladida	Mid Paleo
<i>Cupulocrinus latibrachiatus</i>	GSC 126665g	Vaureal	La Vache	Cone	5.61	6.03	53.4	Dendrocrinida	Cladida	Mid Paleo
<i>Cupulocrinus latibrachiatus</i>	GSC 126665h	Vaureal	La Vache	Cone	6.73	7.18	90.83	Dendrocrinida	Cladida	Mid Paleo
<i>Cupulocrinus latibrachiatus</i>	GSC 126665i	Vaureal	La Vache	Cone	5.69	6.49	62.74	Dendrocrinida	Cladida	Mid Paleo

<i>Cupulocrinus latibrachiatatus</i>	Vaureal	La Vache	Cone		5.84	6.22	59.15	Dendrocrinida	Cladida	Mid Paleo
<i>Cupulocrinus latibrachiatatus</i>	Vaureal	La Vache	Cone		5.02	6.01	47.47	Dendrocrinida	Cladida	Mid Paleo
<i>Cupulocrinus latibrachiatatus</i>	Vaureal	La Vache	Cone		4.65	5.64	38.77	Dendrocrinida	Cladida	Mid Paleo
<i>Cupulocrinus latibrachiatatus</i>	Vaureal	La Vache	Cone		5.13	5.38	38.82	Dendrocrinida	Cladida	Mid Paleo
<i>Cupulocrinus latibrachiatatus</i>	Vaureal	La Vache	Cone		6.08	6.44	66.02	Dendrocrinida	Cladida	Mid Paleo
<i>Cupulocrinus latibrachiatatus</i>	Vaureal	La Vache	Cone		3.65	4.97	23.6	Dendrocrinida	Cladida	Mid Paleo
<i>Cupulocrinus latibrachiatatus</i>	Vaureal	La Vache	Cone		3.04	5.82	26.96	Dendrocrinida	Cladida	Mid Paleo
<i>Cupulocrinus latibrachiatatus</i>	Vaureal	La Vache	Cone		5.9	5.6	48.44	Dendrocrinida	Cladida	Mid Paleo
<i>Cupulocrinus latibrachiatatus</i>	Vaureal	La Vache	Cone		8.38	9.02	178.49	Dendrocrinida	Cladida	Mid Paleo
<i>Cupulocrinus latibrachiatatus</i>	Vaureal	La Vache	Cone		5.45	6.8	65.98	Dendrocrinida	Cladida	Mid Paleo
<i>Cupulocrinus latibrachiatatus</i>	Vaureal	La Vache	Cone		4.51	3.93	18.24	Dendrocrinida	Cladida	Mid Paleo
<i>Cupulocrinus latibrachiatatus</i>	Vaureal	La Vache	Cone		4.29	3.85	16.65	Dendrocrinida	Cladida	Mid Paleo
<i>Cupulocrinus latibrachiatatus</i>	Vaureal	La Vache	Cone		5.13	5.92	47.1	Dendrocrinida	Cladida	Mid Paleo
<i>Plicodendrocrinus observationensis</i>	Vaureal	La Vache	Cone		4.15	3.31	11.9	Dendrocrinida	Cladida	Mid Paleo
<i>Plicodendrocrinus observationensis</i>	Vaureal	La Vache	Cone		2.11	2.5	3.44	Dendrocrinida	Cladida	Mid Paleo
<i>Homalocrinidae Indeterminata</i>	Vaureal	La Vache	Cone		8.58	10.73	258.62			
<i>Pleurocystites anticosienseis</i>	Vaureal	Lavache	Bowl		2.63	3.82	14.55			
<i>Gaurocrinus fimbriatus</i>	Vaureal	La Vache	Bowl		0.79	1.78	1.47	Diplobathrida	Camerata	Early Paleo
<i>Gaurocrinus fimbriatus</i>	Vaureal	La Vache	Bowl		2.7	5.26	38.17	Diplobathrida	Camerata	Early Paleo
<i>Gaurocrinus fimbriatus</i>	Vaureal	La Vache	Bowl		2.63	4.47	23.44	Diplobathrida	Camerata	Early Paleo
<i>Gaurocrinus fimbriatus</i>	Vaureal	La Vache	Bowl		2.57	5.26	38.17	Diplobathrida	Camerata	Early Paleo
<i>Gaurocrinus fimbriatus</i>	Vaureal	La Vache	Bowl		2.3	1.71	1.31	Diplobathrida	Camerata	Early Paleo
<i>Gaurocrinus fimbriatus</i>	Vaureal	La Vache	Bowl		3.42	3.36	9.89	Diplobathrida	Camerata	Early Paleo
<i>Gaurocrinus fimbriatus</i>	Vaureal	La Vache	Bowl		6.51	8.28	148.61	Diplobathrida	Camerata	Early Paleo
<i>Gaurocrinus fimbriatus</i>	Vaureal	La Vache	Bowl		6.81	7.75	121.86	Diplobathrida	Camerata	Early Paleo
<i>Gaurocrinus fimbriatus</i>	Vaureal	La Vache	Cone		8.46	12.41	341.1	Diplobathrida	Camerata	Early Paleo
<i>Gaurocrinus fimbriatus</i>	Vaureal	La Vache	Cone		6.14	7.88	99.81	Diplobathrida	Camerata	Early Paleo
<i>Gaurocrinus fimbriatus</i>	Vaureal	La Vache	Bowl		3.97	6.55	73.57	Diplobathrida	Camerata	Early Paleo
<i>Gaurocrinus fimbriatus</i>	Vaureal	La Vache	Bowl		5.04	6.16	61.19	Diplobathrida	Camerata	Early Paleo
<i>Gaurocrinus fimbriatus</i>	Vaureal	La Vache	Bowl		5.44	5.02	33.12	Diplobathrida	Camerata	Early Paleo
<i>Gaurocrinus fimbriatus</i>	Vaureal	La Vache	Cone		1.04	1.85	0.74	Diplobathrida	Camerata	Early Paleo
<i>Cupulocrinus latibrachiatatus</i>	Vaureal	La Vache	Bowl		6.94	6.48	71.23	Dendrocrinida	Cladida	Mid Paleo
<i>Cupulocrinus latibrachiatatus</i>	Vaureal	La Vache	Cone		6.02	6.47	65.97	Dendrocrinida	Cladida	Mid Paleo
<i>Cupulocrinus latibrachiatatus</i>	Vaureal	La Vache	Bowl		6.71	6.31	65.77	Dendrocrinida	Cladida	Mid Paleo
<i>Cupulocrinus latibrachiatatus</i>	Vaureal	La Vache	Cone		9.9	7.33	139.26	Dendrocrinida	Cladida	Mid Paleo
<i>Cupulocrinus latibrachiatatus</i>	Vaureal	La Vache	Bowl		5.94	8.41	155.72	Dendrocrinida	Cladida	Mid Paleo
<i>Cupulocrinus latibrachiatatus</i>	Vaureal	La Vache	Bowl		3.69	5.64	46.97	Dendrocrinida	Cladida	Mid Paleo
<i>Cupulocrinus latibrachiatatus</i>	Vaureal	La Vache	Cone		9.07	9.7	223.42	Dendrocrinida	Cladida	Mid Paleo
<i>Cupulocrinus latibrachiatatus</i>	Vaureal	La Vache	Cone		6.81	4.57	37.23	Dendrocrinida	Cladida	Mid Paleo
<i>Cupulocrinus latibrachiatatus</i>	Vaureal	La Vache	Cone		5.49	5.02	36.22	Dendrocrinida	Cladida	Mid Paleo
<i>Cupulocrinus latibrachiatatus</i>	Vaureal	La Vache	Bowl		10.13	8.43	156.84	Dendrocrinida	Cladida	Mid Paleo
<i>Pleurocystites anticosienseis</i>	Vaureal	La Vache	Ellipse		26.01	26.58	9832.48			
<i>Pleurocystites anticosienseis</i>	Vaureal	La Vache	Ellipse		22.03	19.29	3758.33			
<i>Plicodendrocrinus observationensis</i>	Vaureal	Tower	Cone		2.89	3.29	8.2	Dendrocrinida	Cladida	Mid Paleo
<i>Carabocrinus boltoni</i>	Vaureal	Homard	Bowl		14.79	19.56	1959.18	Cyathocrinida	Cladida	Mid Paleo
<i>Cildochirus milibayensis</i>	Vaureal	Homard	Cone		4.28	4.4	21.69	Sagenocrinida	Flexibilia	Mid Paleo



<i>Euspirocinus gagnoni</i>	GSC 126712	Ellis Bay	Laframboise	Bowl		2.24	4.61	25.57	Cyathocrinida	Cladida	Mid Paleo
<i>Dendrocinus leptos</i>	GSC 126715	Ellis Bay	Laframboise	Cone		0.79	1.12	0.37	Dendrocinida	Cladida	Mid Paleo
<i>Dendrocinus leptos</i>	GSC 126716	Ellis Bay	Laframboise	Cone		0.79	1.18	0.29	Dendrocinida	Cladida	Mid Paleo
<i>Charactocrinus billingsi</i>	GSC 126684	Ellis Bay	Laframboise	Cone		4.93	4.3	23.86	Calceocrinida	Disparida	Early Paleo
<i>Euspirocinus gagnoni</i>	GSC 126708	Becsclie	Fox Point	Bowl		5.62	11.13	360.96	Cyathocrinida	Cladida	Mid Paleo
<i>Euspirocinus gagnoni</i>	GSC 126709	Becsclie	Fox Point	Bowl		6.41	13.04	580.5	Cyathocrinida	Cladida	Mid Paleo
<i>Protaxocrinus paraios</i>	GSC 126802a	Becsclie	Fox Point	Cone		2.45	2.99	5.73	Taxocrinida	Flexibilia	Mid Paleo
<i>Protaxocrinus paraios</i>	GSC 126802b	Becsclie	Fox Point	Bowl		3.61	5.71	48.74	Taxocrinida	Flexibilia	Mid Paleo
<i>Protaxocrinus paraios</i>	GSC 126802c	Becsclie	Fox Point	Cone		1.32	1.26	0.55	Taxocrinida	Flexibilia	Mid Paleo
<i>Protaxocrinus paraios</i>	GSC 126802d	Becsclie	Fox Point	Cone		2.14	3.04	5.18	Taxocrinida	Flexibilia	Mid Paleo
<i>Protaxocrinus paraios</i>	GSC 126802e	Becsclie	Fox Point	Bowl		3.84	4.64	26.15	Taxocrinida	Flexibilia	Mid Paleo
<i>Allopocrinus parvus</i>	GSC 126806a	Becsclie	Fox Point	Bowl		4.36	5.22	37.24	Monobathrida	Camerata	Mid Paleo
<i>Becsclerinus adonis</i>	GSC 126810a	Becsclie	Fox Point	Cone		0.79	1.58	0.52	Diplobathrida	Camerata	Early Paleo
<i>Becsclerinus adonis</i>	GSC 126810b	Becsclie	Fox Point	Cone		1.84	1.84	1.64	Diplobathrida	Camerata	Early Paleo
<i>Becsclerinus adonis</i>	GSC 126810c	Becsclie	Fox Point	Cone		2.24	2.5	3.66	Diplobathrida	Camerata	Early Paleo
<i>Becsclerinus adonis</i>	GSC 126811a	Becsclie	Fox Point	Bowl		1.53	2.32	3.27	Diplobathrida	Camerata	Early Paleo
<i>Becsclerinus adonis</i>	GSC 126811b	Becsclie	Fox Point	<b>Bowl</b>		4.4	3.57	11.91	Diplobathrida	Camerata	Early Paleo
<i>Becsclerinus adonis</i>	GSC 126811c	Becsclie	Fox Point	Bowl		2.63	4.06	17.52	Diplobathrida	Camerata	Early Paleo
<i>Becsclerinus adonis</i>	GSC 126811d	Becsclie	Fox Point	Bowl		2.07	3.37	10.02	Diplobathrida	Camerata	Early Paleo
<i>Becsclerinus adonis</i>	GSC 126812a	Becsclie	Fox Point	Cone		9.21	7.29	128.14	Diplobathrida	Camerata	Early Paleo
<i>Becsclerinus adonis</i>	GSC 126808b	Becsclie	Chabot	Bowl		1.5	1.77	1.45	Diplobathrida	Camerata	Early Paleo
<i>Becsclerinus adonis</i>	GSC 126860a	Becsclie	Chabot	Cone		1.97	1.32	0.89	Diplobathrida	Camerata	Early Paleo
<i>Dendrocinus leptos</i>	GSC 126860c	Becsclie	Chabot	Cone		2.5	2.11	2.9	Dendrocinida	Cladida	Mid Paleo
<i>Apoarchaeocrinus anticostiensis</i>	GSC 126729a	Becsclie	Chabot	Cone		10.68	11.54	372.35	Diplobathrida	Camerata	Early Paleo
<i>Apoarchaeocrinus anticostiensis</i>	GSC 126729b	Becsclie	Chabot	Cone		21.3	18.33	1873.58	Diplobathrida	Camerata	Early Paleo
<i>Apoarchaeocrinus anticostiensis</i>	GSC 126729d	Becsclie	Chabot	Bowl		9.78	15.75	1022.85	Diplobathrida	Camerata	Early Paleo
<i>Apoarchaeocrinus anticostiensis</i>	GSC 126729e	Becsclie	Chabot	Bowl		16.02	18.44	1641.54	Diplobathrida	Camerata	Early Paleo
<i>Apoarchaeocrinus anticostiensis</i>	GSC 126729f	Becsclie	Chabot	Bowl		22.32	24.96	4071.01	Diplobathrida	Camerata	Early Paleo
<i>Apoarchaeocrinus anticostiensis</i>	GSC 126729g	Becsclie	Chabot	Bowl		12.14	15.54	982.47	Diplobathrida	Camerata	Early Paleo
<i>Emyelodactylus richardsoni</i>	GSC 126746	Gun River	Sandtop	Cone		1.18	1.05	0.34	Myelodactylida	Disparida	Early Paleo
<i>Laurucrinus sandtopensis</i>	GSC 126874a	Gun River	Macgilvray	Cone		0.92	1.05	0.27	Dendrocinida	Cladida	Mid Paleo
<i>Laurucrinus sandtopensis</i>	GSC 126875b	Gun River	Macgilvray	Cone		1.12	1.05	0.32	Dendrocinida	Cladida	Mid Paleo
<i>Laurucrinus sandtopensis</i>	GSC 126875c	Gun River	Macgilvray	Cone		0.66	0.86	0.13	Dendrocinida	Cladida	Mid Paleo
<i>Laurucrinus sandtopensis</i>	GSC 126875d	Gun River	Macgilvray	Cone		0.72	0.79	0.12	Dendrocinida	Cladida	Mid Paleo
<i>Laurucrinus sandtopensis</i>	GSC 126875e	Gun River	Macgilvray	Cone		0.79	1.05	0.23	Dendrocinida	Cladida	Mid Paleo
<i>Laurucrinus sandtopensis</i>	GSC 126875g	Gun River	Macgilvray	Cone		0.79	0.59	0.07	Dendrocinida	Cladida	Mid Paleo
<i>Laurucrinus sandtopensis</i>	GSC 126875i	Gun River	Macgilvray	Bowl		0.79	1.18	0.43	Dendrocinida	Cladida	Mid Paleo
<i>Laurucrinus sandtopensis</i>	GSC 126876	Gun River	Macgilvray	Cone		1.64	2.24	2.15	Dendrocinida	Cladida	Mid Paleo
<i>Stipatocrinus hulverti</i>	GSC 126747	Gun River	MacGilvray	Cone		1.84	3.16	4.81	Monobathrida	Camerata	Mid Paleo
<i>Emyelodactylus springeri</i>	GSC 126745	Jupiter	Goeland	Cone		2.11	1.58	1.37	Myelodactylida	Disparida	Early Paleo
<i>Protaxocrinus sideros</i>	GSC 126764	Jupiter	Goeland	Bowl		3.57	3.86	#VALUE!	Taxocrinida	Flexibilia	Mid Paleo
<i>Protaxocrinus sideros</i>	GSC 126767	Jupiter	Goeland	Bowl		5.49	3.84	14.82	Taxocrinida	Flexibilia	Mid Paleo
<i>Bucurcinus saccus</i>	GSC 126785	Jupiter	Goeland	Cone		24.62	28	5053.27	Diplobathrida	Camerata	Early Paleo
<i>Bucurcinus saccus</i>	GSC 126786	Jupiter	Goeland	Cone		22.83	25.02	3741.53	Diplobathrida	Camerata	Early Paleo
<i>Protaxocrinus paraios</i>	GSC 126800	Jupiter	Goeland	Bowl		5.49	8.39	154.62	Taxocrinida	Flexibilia	Mid Paleo
<i>Dimerocrinittidae indeterminate</i>	GSC 126801	Jupiter	Goeland	Bowl		4.04	5.76	50.03	Diplobathrida	Camerata	Early Paleo

<i>Cybelecrinus iadus</i>	GSC 126820	Jupiter	Goeland	Bowl	10.9	11.94	445.64	Diplobathrida	Camérata	Early Paleo
<i>Cybelecrinus iadus</i>	GSC 126821	Jupiter	Goeland	Bowl	5.68	10.3	286.08	Diplobathrida	Camérata	Early Paleo
<i>Cybelecrinus iadus</i>	GSC 126822	Jupiter	Goeland	Bowl	8.49	15.68	1009.27	Diplobathrida	Camérata	Early Paleo
<i>Protaxocrinus sideros</i>	OSU 32279a	Jupiter	Goeland-East Poi	Cone	3.82	3.98		Taxocrinida	Flexibilia	Mid Paleo
<i>Protaxocrinus sideros</i>	OSU 32279b	Jupiter	Goeland-East Poi	Bowl	5.31	7.15	95.69	Taxocrinida	Flexibilia	Mid Paleo
<i>Fibrocrinus phragmos</i>	GSC 126769	Jupiter	East Point	Bowl	12.69	17.08	1304.46	Monobathrida	Camérata	Mid Paleo
<i>Fibrocrinus phragmos</i>	GSC 126770	Jupiter	East Point	Bowl	16.09	24.73	3959.5	Monobathrida	Camérata	Mid Paleo
<i>Fibrocrinus phragmos</i>	GSC 126771	Jupiter	East Point	Bowl	15.81	24.2	3710.35	Monobathrida	Camérata	Mid Paleo
<i>Fibrocrinus phragmos</i>	GSC 126772	Jupiter	East Point	Bowl	18.37	23.59	3436.78	Monobathrida	Camérata	Mid Paleo
<i>Fibrocrinus phragmos</i>	GSC 126773	Jupiter	East Point	Bowl	7.62	12.64	528.7	Monobathrida	Camérata	Mid Paleo
<i>Fibrocrinus phragmos</i>	GSC 126774	Jupiter	East Point	Bowl	10.82	18.32	1609.7	Monobathrida	Camérata	Mid Paleo
<i>Fibrocrinus phragmos</i>	GSC 126775	Jupiter	East Point	Bowl	20.42	19.29	1879.17	Monobathrida	Camérata	Mid Paleo
<i>Fibrocrinus phragmos</i>	GSC 126776	Jupiter	East Point	Bowl	8.53	12.32	489.55	Monobathrida	Camérata	Mid Paleo
<i>Fibrocrinus phragmos</i>	GSC 126777	Jupiter	East Point	Bowl	13.07	23.82	3538.29	Monobathrida	Camérata	Mid Paleo
<i>Fibrocrinus phragmos</i>	GSC 126778	Jupiter	East Point	Bowl	16.01	18.24	1588.7	Monobathrida	Camérata	Mid Paleo
<i>Fibrocrinus phragmos</i>	GSC 126779	Jupiter	East Point	Bowl	13.34	15.93	1058.32	Monobathrida	Camérata	Mid Paleo
<i>Horocrinus quebecensis</i>	GSC 126781	Jupiter	East Point	Bowl	3.24	6.41	68.95	Sagenocrinida	Flexibilia	Mid Paleo
<i>Ladacrinus asynaptos</i>	GSC 126782	Jupiter	East Point	Bowl	5.94	9.78	244.9	Taxocrinida	Flexibilia	Mid Paleo
<i>Ladacrinus asynaptos</i>	GSC 126796	Jupiter	East Point	Cone	8.36	10.17	226.37	Taxocrinida	Flexibilia	Mid Paleo
<i>Ladacrinus asynaptos</i>	GSC 126797a	Jupiter	East Point	Bowl	9.6	15.05	892.44	Taxocrinida	Flexibilia	Mid Paleo
<i>Ladacrinus asynaptos</i>	GSC 126797b	Jupiter	East Point	Bowl	6.72	8.91	185.18	Taxocrinida	Flexibilia	Mid Paleo
<i>Ladacrinus asynaptos</i>	GSC 126797c	Jupiter	East Point	Bowl	10.77	11.36	383.8	Taxocrinida	Flexibilia	Mid Paleo
<i>Fibrocrinus phragmos</i>	GSC 126869a	Jupiter	East Point	Bowl	18.06	21.54	2616.41	Monobathrida	Camérata	Mid Paleo
<i>Fibrocrinus phragmos</i>	GSC 126869b	Jupiter	East Point	Bowl	15.55	17.56	1417.56	Monobathrida	Camérata	Mid Paleo
<i>Fibrocrinus phragmos</i>	GSC 126870a	Jupiter	East Point	Bowl	16.3	22.06	2810.51	Monobathrida	Camérata	Mid Paleo
<i>Fibrocrinus phragmos</i>	GSC 126871	Jupiter	East Point	Bowl	11.47	15.38	952.44	Monobathrida	Camérata	Mid Paleo
<i>Fibrocrinus phragmos</i>	GSC 126872	Jupiter	East Point	Bowl	18.33	26.48	4860.96	Monobathrida	Camérata	Mid Paleo
<i>Fibrocrinus phragmos</i>	GSC 126873	Jupiter	East Point	Cone	13	15.43	810.3	Monobathrida	Camérata	Mid Paleo
<i>Fibrocrinus phragmos</i>	GSC 126873a	Jupiter	East Point	Bowl	10.87	19.08	1818.46	Monobathrida	Camérata	Mid Paleo
<i>Fibrocrinus phragmos</i>	GSC 126873b	Jupiter	East Point	Bowl	7	13.42	632.74	Monobathrida	Camérata	Mid Paleo
<i>Fibrocrinus phragmos</i>	GSC 126873c	Jupiter	East Point	Bowl	10.22	16.73	1225.9	Monobathrida	Camérata	Mid Paleo
<i>Dendrocrinus sp.</i>	GSC 126818	Jupiter	Richardson	Cone	0.39	0.53	0.03	Dendrocrinida	Cladida	Mid Paleo
<i>Fraguicrinus bothros</i>	GSC 126881	Jupiter	Richardson	Cone	4.7	4.09				
<i>Fibrocrinus phragmos</i>	OSU 32288a	Jupiter	East Point	Ellipsee	8.51	14.72	1670.02	Monobathrida	Camérata	Mid Paleo
<i>Fibrocrinus phragmos</i>	OSU 32289a	Jupiter	East Point	Cone	7.55	6.82	91.94	Monobathrida	Camérata	Mid Paleo
<i>Fibrocrinus phragmos</i>	OSU 32289c	Jupiter	East Point	Cone	13.57	12.41	547.13	Monobathrida	Camérata	Mid Paleo
<i>Fibrocrinus phragmos</i>	OSU 32289d	Jupiter	East Point	Cone	13.99	15.76	909.7	Monobathrida	Camérata	Mid Paleo
<i>Fibrocrinus phragmos</i>	OSU 32289e	Jupiter	East Point	Ellipsee	13.66	27.05	10363.35	Monobathrida	Camérata	Mid Paleo
<i>Fibrocrinus phragmos</i>	OSU 32290b	Jupiter	East Point	Ellipsee	13.93	17.45	2782.18	Monobathrida	Camérata	Mid Paleo
<i>Fibrocrinus phragmos</i>	OSU 32291	Jupiter	East Point	Cone	17.14	17.43	1363.24	Monobathrida	Camérata	Mid Paleo
<i>Fibrocrinus phragmos</i>	OSU 32292a	Jupiter	East Point	Bowl	8.4	13.14	593.96	Monobathrida	Camérata	Mid Paleo
<i>Fibrocrinus phragmos</i>	OSU 32293	Jupiter	East Point	Cone	18.11	17.77	1497.14	Monobathrida	Camérata	Mid Paleo
<i>Fibrocrinus phragmos</i>	OSU Z041a	Jupiter	East Point	Bowl	11.48	17.66	1441.92	Monobathrida	Camérata	Mid Paleo
<i>Fibrocrinus phragmos</i>	OSU Z041b	Jupiter	East Point	Bowl	10.49	17.55	1415.14	Monobathrida	Camérata	Mid Paleo
<i>Fibrocrinus phragmos</i>	OSU Z041d	Jupiter	East Point	Bowl	15.54	14.55	806.41	Monobathrida	Camérata	Mid Paleo
<i>Protaxocrinus sideros</i>	GSC 126883	Jupiter	Cybele	Cone	3.05	3.6	10.35	Taxocrinida	Flexibilia	Mid Paleo

<i>Protaxocrinus sideros</i>	GSC 126766	Jupiter	Cybele	Bowl	2.71	2.74	5.39	Taxocrinida	Flexibilia	Mid Paleo
<i>Dimerocrinites elegans</i>	GSC 126724	Jupiter	Cybele	Cone	2.89	4.06	12.47	Diplobathrida	Camerata	Early Paleo
<i>Protaxocrinus sideros</i>	GSC 126763	Jupiter	Cybele	Bowl	3.15	4.02	17.01	Taxocrinida	Flexibilia	Mid Paleo
<i>Aetocrinus gracilis</i>	GSC 126814a	Jupiter	Cybele	Cone	1.45	1.58	0.94	Dendrocrinida	Cladida	Mid Paleo
<i>Aetocrinus gracilis</i>	GSC 126814b	Jupiter	Cybele	Cone	1.18	1.84	1.05	Dendrocrinida	Cladida	Mid Paleo
<i>Aetocrinus gracilis</i>	GSC 126814c	Jupiter	Cybele	Cone	0.92	1.18	0.34	Dendrocrinida	Cladida	Mid Paleo
<i>Aetocrinus gracilis</i>	GSC 126814d	Jupiter	Cybele	Cone	1.05	1.32	0.48	Dendrocrinida	Cladida	Mid Paleo
<i>Aetocrinus gracilis</i>	GSC 126814e	Jupiter	Cybele	Cone	1.58	1.58	1.03	Dendrocrinida	Cladida	Mid Paleo
<i>Aetocrinus gracilis</i>	GSC 126814g	Jupiter	Cybele	Cone	1.91	1.71	1.46	Dendrocrinida	Cladida	Mid Paleo
<i>Cybelecrinus ladus</i>	GSC 126823	Jupiter	Cybele	Bowl	6.88	11.96	447.88	Diplobathrida	Camerata	Early Paleo
<i>Protaxocrinus sideros</i>	OSU 32281	Jupiter	Cybele	Bowl	4.13	4.2	19.4	Taxocrinida	Flexibilia	Mid Paleo
<i>Cybelecrinus nebrus</i>	GSC 126825	Jupiter	Cybele	Bowl	7.16	10.39	293.64	Diplobathrida	Camerata	Early Paleo
<i>Dimerocrinites elegans</i>	GSC 126748	Jupiter	Ferrum	Cone	4.6	4.23	21.55	Diplobathrida	Camerata	Early Paleo
<i>Dimerocrinites elegans</i>	GSC 126749	Jupiter	Ferrum	Cone	5.19	4.73	30.4	Diplobathrida	Camerata	Early Paleo
<i>Dimerocrinites elegans</i>	GSC 126750	Jupiter	Ferrum	Cone	5.9	5.79	51.78	Diplobathrida	Camerata	Early Paleo
<i>Dimerocrinites elegans</i>	GSC 126751	Jupiter	Ferrum	Cone	4.95	5.47	38.77	Diplobathrida	Camerata	Early Paleo
<i>Dimerocrinites elegans</i>	GSC 126752	Jupiter	Ferrum	Cone	7.63	8.27	136.62	Diplobathrida	Camerata	Early Paleo
<i>Dimerocrinites elegans</i>	GSC 126753	Jupiter	Ferrum	Cone	6.33	4.75	37.38	Diplobathrida	Camerata	Early Paleo
<i>Dimerocrinites elegans</i>	GSC 126754	Jupiter	Ferrum	Cone	5.46	5.3	40.15	Diplobathrida	Camerata	Early Paleo
<i>Dimerocrinites elegans</i>	GSC 126755	Jupiter	Ferrum	Cone	6.15	8.31	111.18	Diplobathrida	Camerata	Early Paleo
<i>Dimerocrinites elegans</i>	GSC 126756	Jupiter	Ferrum	Cone	5.96	5.09	40.43	Diplobathrida	Camerata	Early Paleo
<i>Dimerocrinites elegans</i>	GSC 126757	Jupiter	Ferrum	Bowl	3.56	7.49	110.01	Diplobathrida	Camerata	Early Paleo
<i>Protaxocrinus sideros</i>	GSC 126758	Jupiter	Ferrum	Cone	2.68	3.12	6.83	Taxocrinida	Flexibilia	Mid Paleo
<i>Protaxocrinus sideros</i>	GSC 126759	Jupiter	Ferrum	Bowl	4.02	5.92	54.32	Taxocrinida	Flexibilia	Mid Paleo
<i>Protaxocrinus sideros</i>	GSC 126760	Jupiter	Ferrum	Bowl	7.58	9.78	244.9	Taxocrinida	Flexibilia	Mid Paleo
<i>Protaxocrinus sideros</i>	GSC 126761	Jupiter	Ferrum	Bowl	2.36	4.38	22	Taxocrinida	Flexibilia	Mid Paleo
<i>Protaxocrinus sideros</i>	GSC 126762	Jupiter	Ferrum	Bowl	2.93	3.25	8.99	Taxocrinida	Flexibilia	Mid Paleo
<i>Jovacrinus spinosus</i>	GSC 126787	Jupiter	Ferrum	Bowl	4.72	9.52	225.88	Monobathrida	Camerata	Mid Paleo
<i>Jovacrinus spinosus</i>	GSC 126788b	Jupiter	Ferrum	Bowl	3.49	6.82	83.05	Monobathrida	Camerata	Mid Paleo
<i>Jovacrinus spinosus</i>	GSC 126788c	Jupiter	Ferrum	Bowl	2.79	4.89	30.61	Monobathrida	Camerata	Mid Paleo
<i>Cybelecrinus ladus</i>	GSC 126788f	Jupiter	Ferrum	Bowl	2.59	5.08	34.32	Diplobathrida	Camerata	Early Paleo
<i>Eucalyptocrinus sp.</i>	GSC 126788g	Jupiter	Ferrum	Bowl	1.36	7.29	101.43	Monobathrida	Camerata	Mid Paleo
<i>Jovacrinus spinosus</i>	GSC 126789a	Jupiter	Ferrum	Bowl	4.29	4.48	23.54	Monobathrida	Camerata	Mid Paleo
<i>Jovacrinus spinosus</i>	GSC 126789d	Jupiter	Ferrum	Bowl	2.79	6.17	61.49	Monobathrida	Camerata	Mid Paleo
<i>Jovacrinus spinosus</i>	GSC 126789f	Jupiter	Ferrum	Bowl	4.26	4.94	31.56	Monobathrida	Camerata	Mid Paleo
<i>Jovacrinus spinosus</i>	GSC 126789g	Jupiter	Ferrum	Bowl	1.14	3.62	12.42	Monobathrida	Camerata	Mid Paleo
<i>Jovacrinus spinosus</i>	GSC 126790b	Jupiter	Ferrum	Cone	3.46	3.65	12.07	Monobathrida	Camerata	Mid Paleo
<i>Jovacrinus spinosus</i>	GSC 126790c	Jupiter	Ferrum	Cone	2.67	3.18	7.07	Monobathrida	Camerata	Mid Paleo
<i>Cybelecrinus ladus</i>	GSC 126819	Jupiter	Ferrum	Bowl	7.06	12.61	524.94	Diplobathrida	Camerata	Early Paleo
<i>Jovacrinus lugum</i>	GSC 126824a	Jupiter	Ferrum	Cone	3.36	3.62	11.53	Monobathrida	Camerata	Mid Paleo
<i>Jovacrinus lugum</i>	GSC 126824b	Jupiter	Ferrum	Cone	2.3	4.17	10.47	Monobathrida	Camerata	Mid Paleo
<i>Jovacrinus lugum</i>	GSC 126824c	Jupiter	Ferrum	Cone	2	4.08	8.72	Monobathrida	Camerata	Mid Paleo
<i>Jovacrinus lugum (fragment)</i>	GSC 126824d	Jupiter	Ferrum	Bowl	2.89	4.76	28.24	Monobathrida	Camerata	Mid Paleo
<i>Jovacrinus spinosus</i>	GSC 126790f	Jupiter	Ferrum	Cone	3.47	4.96	22.35	Monobathrida	Camerata	Mid Paleo
<i>Chenocrinus canadensis</i>	GSC 126826a	Jupiter	Ferrum	Cone	1.66	2.16	2.03	Monobathrida	Camerata	Mid Paleo
<i>Chenocrinus canadensis</i>	GSC 126826b	Jupiter	Ferrum	Cone	1.63	1.88	1.51	Monobathrida	Camerata	Mid Paleo

<i>Protaxocrinus sideros</i>	GSC 126863	Jupiter	Ferrum	Bowl		1.6	2.11	2.46	Taxocrinida	Flexibila	Mid Paleo
<i>Dimerocrinites elegans</i>	OSU 32275a	Jupiter	Ferrum	Cone		4.74	5.14	32.78	Diplobathrinda	Camerata	Early Paleo
<i>Dimerocrinites elegans</i>	OSU 32275b	Jupiter	Ferrum	Cone		3.36	3.35	9.87	Diplobathrinda	Camerata	Early Paleo
<i>Dimerocrinites elegans</i>	OSU 32275c	Jupiter	Ferrum	Bowl		2.55	4.33	21.25	Diplobathrinda	Camerata	Early Paleo
<i>Dimerocrinites elegans</i>	OSU 32275f	Jupiter	Ferrum	Bowl		7.43	9.7	238.94	Diplobathrinda	Camerata	Early Paleo
<i>Dimerocrinites elegans</i>	OSU 32275i	Jupiter	Ferrum	Bowl		6.4	8.5	160.78	Diplobathrinda	Camerata	Early Paleo
<i>Dimerocrinites elegans</i>	OSU 32275k	Jupiter	Ferrum	Cone		7.12	7.95	117.81	Diplobathrinda	Camerata	Early Paleo
<i>Dimerocrinites elegans</i>	OSU 32276	Jupiter	Ferrum	Cone		6.43	5.36	48.36	Diplobathrinda	Camerata	Early Paleo
<i>Dimerocrinites elegans</i>	OSU 32277	Jupiter	Ferrum	Cone		4.56	2.89	9.97	Diplobathrinda	Camerata	Early Paleo
<i>Dimerocrinites elegans</i>	OSU 32278	Jupiter	Ferrum	Bowl		7.66	8.32	150.78	Diplobathrinda	Camerata	Early Paleo
<i>Protaxocrinus sideros</i>	OSU 32280	Jupiter	Ferrum	Cone		5.41	7.75	85.07	Taxocrinida	Flexibila	Mid Paleo
<i>Jovacrinus spinosus</i>	OSU 32283a	Jupiter	Ferrum	Bowl		4.56	7.95	131.54	Monobathrinda	Camerata	Mid Paleo
<i>Jovacrinus spinosus</i>	OSU 32283b	Jupiter	Ferrum	Bowl		9.58	10.21	278.64	Monobathrinda	Camerata	Mid Paleo
<i>Jovacrinus spinosus</i>	OSU 32283c	Jupiter	Ferrum	Bowl		5.06	5.9	53.77	Monobathrinda	Camerata	Mid Paleo
<i>Jovacrinus spinosus</i>	OSU 32284a	Jupiter	Ferrum	Bowl		6.33	9.13	199.24	Monobathrinda	Camerata	Mid Paleo
<i>Jovacrinus jugum</i>	OSU 32295a	Jupiter	Ferrum	Bowl		1.87	2.86	6.12	Monobathrinda	Camerata	Mid Paleo
<i>Laurocrinus sandtloperensis</i>	GSC 126817a	Jupiter	Pavillon	Cone		1.32	2.11	1.53	Dendrocrinida	Cladida	Mid Paleo
<i>Ladacrinus? sp.</i>	GSC 126784	Chicotte	Telychian	Bowl		6.55	17.11	1311.35	Dendrocrinida	Cladida	Mid Paleo
<i>Convucrinus schucherti</i>	GSC 126828	Chicotte	Telychian	Cone		11.22	11.62	396.62	Calceocrinida	Disparida	Early Paleo
<i>Dendrocrinus sp.</i>	GSC 126816	Chicotte	Telychian	Cone		5.52	4.51	29.39	Dendrocrinida	Cladida	Mid Paleo
<i>Leviyathocrinites sablensis</i>	GSC 126829	Chicotte	Telychian	Cone		12.44	13.01	551.24	Cyathocrinida	Cladida	Mid Paleo
<i>Abacocrinus latus</i>	GSC 126831	Chicotte	Telychian	Cone		23.57	27.88	4727.81	Monobathrinda	Camerata	Mid Paleo
<i>Abatocrinus latus</i>	GSC 126832	Chicotte	Telychian	Cone		33	39.25	13309.49	Monobathrinda	Camerata	Mid Paleo
<i>Abatocrinus latus</i>	GSC 126833	Chicotte	Telychian	Cone		34.54	39.32	13980.34	Monobathrinda	Camerata	Mid Paleo
<i>Abatocrinus latus</i>	GSC 126834	Chicotte	Telychian	Cone		13.96	17.21	1082.47	Monobathrinda	Camerata	Mid Paleo
<i>Abatocrinus latus</i>	GSC 126835	Chicotte	Telychian	Bowl		13.94	19.9	2063.13	Monobathrinda	Camerata	Mid Paleo
<i>Abatocrinus latus</i>	GSC 126836	Chicotte	Telychian	Bowl		15.91	21.12	2466.32	Monobathrinda	Camerata	Mid Paleo
<i>Abatocrinus latus</i>	GSC 126837	Chicotte	Telychian	Cone		19.07	19.04		Monobathrinda	Camerata	Mid Paleo
<i>Abacocrinus latus</i>	GSC 126838	Chicotte	Telychian	Cone		14.43	17.79		Monobathrinda	Camerata	Mid Paleo
<i>Abacocrinus sp. A</i>	GSC 126839	Chicotte	Telychian	Bowl		15.87	22.42	2950.36	Monobathrinda	Camerata	Mid Paleo
<i>Abacocrinus sp. A</i>	GSC 126841	Chicotte	Telychian	Cone		35.27	35.4		Monobathrinda	Camerata	Mid Paleo
<i>Abacocrinus sp.</i>	GSC 126842	Chicotte	Telychian	Cone		23.21	25.35		Monobathrinda	Camerata	Mid Paleo
<i>Abacocrinus sp. A</i>	GSC 126843a	Chicotte	Telychian	Bowl		11.21	18.89	1764.67	Monobathrinda	Camerata	Mid Paleo
<i>Abacocrinus sp. A</i>	GSC 126843b	Chicotte	Telychian	Bowl		12.45	20.2	2157.86	Monobathrinda	Camerata	Mid Paleo
<i>Abacocrinus sp. A</i>	GSC 126843c	Chicotte	Telychian	Bowl		22.76	29.7	6858.63	Monobathrinda	Camerata	Mid Paleo
<i>Abacocrinus sp. A</i>	GSC 126843d	Chicotte	Telychian	Bowl		9.42	21.89	2746.03	Monobathrinda	Camerata	Mid Paleo
<i>Abacocrinus sp. B</i>	GSC 126844	Chicotte	Telychian	Ellipse		17.13	13.68	1340.47	Monobathrinda	Camerata	Mid Paleo
<i>Abacocrinus sp. B</i>	GSC 126845	Chicotte	Telychian	Bowl		20.46	24.88	4031.99	Monobathrinda	Camerata	Mid Paleo
<i>Abacocrinus sp. B</i>	GSC 126846	Chicotte	Telychian	Bowl		14.53	18.1	1552.4	Monobathrinda	Camerata	Mid Paleo
<i>Abacocrinus sp. B</i>	GSC 126847	Chicotte	Telychian	Bowl		15.35	20.16	2145.06	Monobathrinda	Camerata	Mid Paleo
<i>Abacocrinus sp. B</i>	GSC 126848a	Chicotte	Telychian	Bowl		12.64	24.65	3921.2	Monobathrinda	Camerata	Mid Paleo
<i>Eucalyptocrinites? Sp.</i>	GSC 126849	Chicotte	Telychian	Bowl		36.05	36.88	13132.31	Monobathrinda	Camerata	Mid Paleo
<i>Eucalyptocrinus sp.</i>	GSC 126852	Chicotte	Telychian	Cone		18.35	23.43	2637.24	Monobathrinda	Camerata	Mid Paleo
<i>Myosocrinus Chicottensis</i>	GSC 126854	Chicotte	Telychian	Bowl		16.28	14.7	831.61	Dendrocrinida	Cladida	Mid Paleo
<i>Myosocrinus Chicottensis</i>	GSC 126855	Chicotte	Telychian	Ellipse		9.1	18.09	3099.66	Dendrocrinida	Cladida	Mid Paleo
<i>Lecanocrinidae? Indeterminate</i>	GSC 126856	Chicotte	Telychian	Cone		18.52	12.51	758.79	Sagenocrinida	Flexibila	Mid Paleo

<i>Allozygocrinus exallos</i>	GSC 126857	Chicotte	Telychian	Cone	23.59	23.19	3321.22	Diplobathrida	Camerata	Early Paleo
Rhondocrinitidae Indeterminate	GSC 126859	Chicotte	Telychian	Ellipse	27.27	47.32	55479.49	Diplobathrida	Camerata	Early Paleo
<i>Abacocrinus latus</i>	OSU 32296a	Chicotte	Telychian	Cone	18.98	22.5	2515.53	Monobathrida	Camerata	Mid Paleo
<i>Abacocrinus latus</i>	OSU 32296b	Chicotte	Telychian	Cone	27.58	26.5	5070.54	Monobathrida	Camerata	Mid Paleo
<i>Abacocrinus latus</i>	OSU 32296c	Chicotte	Telychian	Cone	27.74	23.73	4089.5	Monobathrida	Camerata	Mid Paleo
<i>Abacocrinus latus</i>	OSU 32296d	Chicotte	Telychian	Bowl	15.78	19.22	1858.78	Monobathrida	Camerata	Mid Paleo
<i>Abacocrinus latus</i>	OSU 32296e	Chicotte	Telychian	Bowl	12.32	16.52	1180.32	Monobathrida	Camerata	Mid Paleo
<i>Abacocrinus latus</i>	OSU 32296f	Chicotte	Telychian	Cone	24.2	22.68	3258.89	Monobathrida	Camerata	Mid Paleo
<i>Abacocrinus latus</i>	OSU 32296g	Chicotte	Telychian	Bowl	19.76	19.57	1962.19	Monobathrida	Camerata	Mid Paleo
<i>Abacocrinus latus</i>	OSU 32296h	Chicotte	Telychian	Cone	15.69	13.75	776.6	Monobathrida	Camerata	Mid Paleo
<i>Abacocrinus</i> sp. A	OSU 32297a	Chicotte	Telychian	Bowl	13.89	14.57	809.74	Monobathrida	Camerata	Mid Paleo
<i>Abacocrinus</i> sp. A	OSU 32297b	Chicotte	Telychian	Bowl	12.42	21.82	2719.77	Monobathrida	Camerata	Mid Paleo
<i>Abacocrinus</i> sp. A	OSU 32297c	Chicotte	Telychian	Bowl	22.18	30.36	7326.11	Monobathrida	Camerata	Mid Paleo
<i>Abacocrinus</i> sp. A	OSU 32297d	Chicotte	Telychian	Cone	12.77	14.71	723.41	Monobathrida	Camerata	Mid Paleo

## *References*

- Ausich, W.I. 1980. A model for niche differentiation in Lower Mississippian crinoid communities. *Journal of Paleontology*. 54: 273-288.
- Ausich, W.I. and P. Copper. *In progress*. Anticosti Island Crinoid Monograph. pg 7-25.
- Ausich, W.I., T.W. Kammer, T.K. Baumiller, 1994. Demise of the middle Paleozoic crinoid fauna: a single extinction event or rapid faunal turnover?. *Paleobiology* 20: 345-361.
- Ausich, W.I. and S.E. Peters. 2005. A revised macroevolutionary history for Ordovician-Early Silurian crinoids. *Paleobiology* 31: 538-551.
- Ausich, W.I. 2007. Is it time to quit? 2007 GSA Annual Meeting Abstracts with Programs 228-1.
- Berry, W.B.N., Boucot, A.J. 1973. Glacioeustatic control of Late Ordovician-Early Silurian platform sedimentation and faunal change. *Bulletin of Geological Society of America*, 84, 275-284.
- Borths, M. R. and W. I. Ausich. 2007. Crinoids in Lilliput: Morphological Change in the Class Crinoidea Across the Ordovician –Silurian Boundary. 2007 GSA Annual Meeting Abstracts with Programs 39: 6.
- Brenchley, P. J. 1989. The Late Ordovician Extinction pg 104-132 in S.K. Donovan (ed.), *Mass Extinctions: Processes and evidence*. Columbia University Press, New York.
- Brower, J. C., Clement, C. R. and Veinus, J. 1978. Multivariate analysis of allometry using morphometric measurements. In Merriam, D. F., ed, *Recent advances in geomathematics an international symposium*: New York, Pergamon Press, p. 61-80.
- Donovan, S.K. 1983. Evolution and biostratigraphy of pelmatozoan columnals from the Cambrian and Ordovician of Britain. PhD. Thesis. University of Liverpool.
- Desrochers, A. 2006. Rocky shoreline deposits in the Lower Silurian (upper Llandovery, Telychian) Chicotte Formation, Anticosti Island, Quebec. *Canadian Journal of Earth Sciences*, 43: 8.
- Duke, W.L. 1985. Hummocky cross-stratification, tropical hurricanes and intense winter storms. *Sedimentology*, 32: 167-194.
- Donovan, S.K. 1989 The significance of the British Ordovician crinoid fauna. *Modern Geology* 13: 243-255.
- Eckert, J.D. 1988. Late Ordovician extinction of North American and British crinoids. *Lethaia* 21: 147-167.

Hallam, A. and P.B. Wignall. 1997. Latest Ordovician Extinctions: one disaster after another pg. 39-57 in *Mass Extinctions and Their Aftermath*. Oxford University Press: New York.

Hammer, Ø., Harper, D.A.T., and P. D. Ryan, 2001. PAST: Paleontological Statistics Software Package for Education and Data Analysis. *Palaeontologia Electronica* 4(1): 9pp. <[http://palaeo-electronica.org/2001\\_1/past/issue1\\_01.htm](http://palaeo-electronica.org/2001_1/past/issue1_01.htm)>

Hess, H., W.I. Ausich, C.E. Brett, and M.J. Simms. 1999. *Fossil Crinoids*. Cambridge University Press: Cambridge.

Hone, D.W.E., T.M. Keeseey, D. Pisani and A. Purvis. 2005. Macroevolutionary trends in Dinosauria: Cope's Rule. *Journal of Evolutionary Biology*. 18: 587-595.

Hone, D.W.E. and M.J. Benton. 2005. The evolution of large size: how does Cope's Rule work? *Trends in Ecology and Evolution*. 20: 4-7.

Hone, D.W.E. and M.J. Benton. 2007. Cope's Rule in the Pterosauria and differing perceptions of Cope's Rule at differing taxonomic levels. *Journal of Evolutionary Biology*. 20: 1164-1170.

Lavoie, D., E. Burden, and D. Lebel. 2003. Stratigraphic framework for the Cambro-Ordovician rift and passive margin successions from southern Quebec to western Newfoundland. *Canadian Journal of Earth Sciences*, 40: 177-205.

Le Heron, D. P. and J. Craig. 2008. First-order reconstructions of a Late Ordovician Saharan ice sheet. *Journal of the Geological Society of London*. 165(1): 19-29.

Long, D.G.F. 2007. Tempestite frequency curves: a key to Late Ordovician and Early Silurian subsidence, sea level change, and orbital forcing in the Anticosti foreland basin, Quebec, Canada. *NRC Canada*, 44: 413-431.

Long, D.G.F. and P. Copper. 1994. The Late Ordovician –Early Silurian carbonate tract of Anticosti Island, Gulf of St. Lawrence, Eastern Canada. Geological Association of Canada, Mineralogical Association of Canada, Joint Annual Meeting, Waterloo, Ontario 20-25 May 1994. Field Trip Guidebook B4.

McKerrow, W.S. 1979. Ordovician and Silurian Changes in sea level. *Journal of the Geological Society*, 136, 137-146.

Novack-Gottshall, P.M. and M.A. Lanier. 2008. Scale-dependence of Cope's rule in body size evolution of Paleozoic brachiopods. *Proceedings of the National Academy of Sciences*. 105: 5430-5434.

Peters, S.E. and W.I. Ausich. 2008. A sampling-adjusted macroevolutionary history for Ordovician-Early Silurian crinoids. *Paleobiology* 34: 104-116.

- Poulin, R. 1995. Evolutionary influences on body size in free-living and parasitic isopods. *Biological Journal of the Linnean Society*, 54: 231-244.
- Pruss, S., F. A. Corsetti, and D.J. Bottjer. 2005. The unusual sedimentary record of the Early Triassic: a case study from the southwestern United States. *Paleogeography, Paleoclimatology, Paleoecology*, 222: 33-52.
- Sepkoski, J. J., Jr. 1981. A factor analytic description of the marine fossil record. *Paleobiology* 7:36-53.
- Stockmal, G.S., Waldron, J.W.F. and Quinlan, G.M. 1995. Flexural modeling of Paleozoic foreland basin subsidence, offshore western Newfoundland; evidence for substantial post-Taconian thrust transport. *Journal of Geology*, 103: 653-671.
- Urbanek, A. 1993. Biotic Crises in the history of Upper Silurian graptoloids: a paleobiological model. *Historical Biology* 7: 29-50.
- Waldron, J.W.F., S.D. Anderson, P.A. Carwood, L.B. Goodwin, J. Hall, R.A. Jamieson, S.E. Palmer, G.S. Stockmal and P.F. Williams. 1998. Evolution of the Appalachian Laurentian margin: Lithoprobe results in western Newfoundland. *Canadian Journal of Earth Sciences*, 35: 1271-1287.
- Weihong, H., Shi, G.R. Feng, Q, Campi, M.J. Gu, S., Bu, J, Peng, Y. and Meng, Y. 2006. Brachiopod miniaturization and its possible causes during the Permian-Triassic crisis in deep water environments, South China. *Palaeogeography, Palaeoclimatology, Palaeoecology*, 252: 145-163.
- Wilde, P. 1991. Oceanography in the Ordovician. *In Advances in Ordovician geology*. Edited by C.R. Barnes and S.H. Williams. Geological survey of Canada, Paper 90-9, pp. 283 – 298.